# IMPLEMENTATION OF A GENERIC MEMBRANE-BASED SYSTEM FOR BENEFICIATION AND TREATMENT OF AGRO-INDUSTRIAL WASTEWATER

CJ Garcin • SG Burton

WRC Report No. KV 186/07

Water Research Commission

# Experimental Measurement of Specific Storativity by the Determination of Rock Elastic Parameters

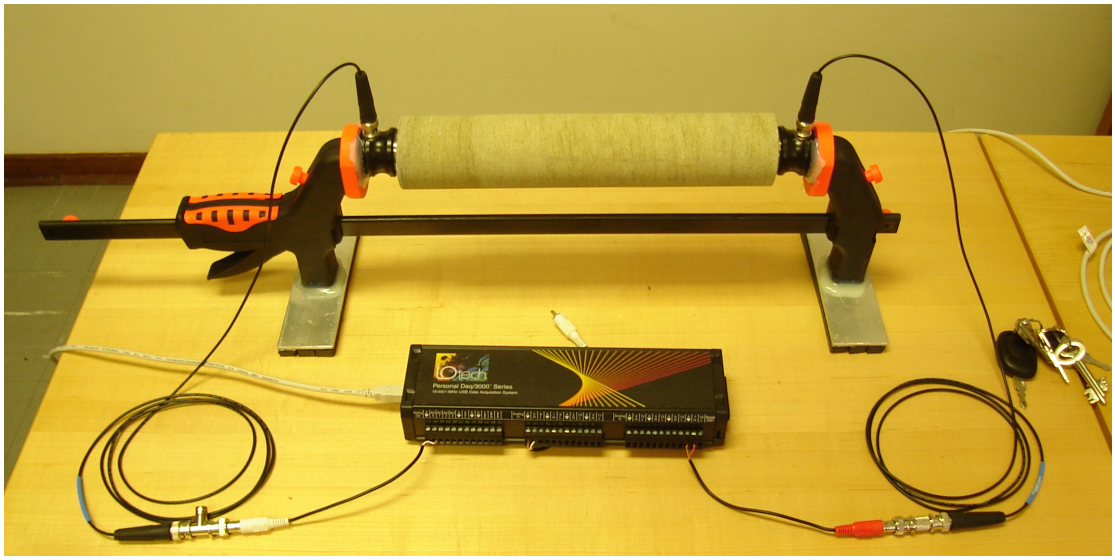

**M du Preez, R Dennis & GJ van Tonder**

**Institute for Groundwater Studies**
**University of the Free State**

**WRC Report No KV 184/07**
**ISBN 978-1-77005-542-1**

**May 2007**

The publication of this report emanates from a consultancy entitled *"Determination of S-values in the Karoo aquifers through the use of resonant ultrasound spectroscopy"* (WRC consultancy K8/643).`

# Executive Summary

As groundwater becomes ever more important as a viable source of fresh water in arid and/or remote areas where surface water supplies are insufficient to sustain life, agriculture and industry, it has become important to accurately estimate, manage and monitor this valuable resource. Much has been done to improve the management of this valuable resource by the development of numerical models that give a realistic estimate on how groundwater reserves will react to changing circumstances in groundwater conditions. The accuracy of these predictions is limited to the effective accuracy of the predictive model, which in turn rely on accurate data on all the variables which will affect the flow of groundwater.

This paper presents a method developed by the authors to determine storativity by determining actual specific storativity values of the rock that make up an aquifer. Storativity is one of the hydrological parameters which affect the flow of groundwater as well as the outcome of predictive models. Storativity is an ambiguous parameter in that it is dependent on two unknown variables, namely aquifer thickness and rock elastic parameters. At present, storativity is estimated using borehole pump test data and inverse modelling, which is not always an accurate measure of the parameter.

Specific storativity is the parameter which specifies the amount of water released by a rock sample when exposed to a change in pressure head, as is the case when a confined aquifer is mined. Specific storativity is determined by experimentally measuring the elastic parameters of a rock sample, in this case, a core sample. These measurements are done in two ways. The first is to measure the compressive and shear wave velocities of the rock by inducing an ultrasonic pulse into one side of the core sample and measuring the time it takes the pulse to travel through the sample. The travel times are then converted into compressive and shear velocities which in turn are used to determine the bulk modulus and shear modulus of the sample. The second method involves using resonant ultrasound spectrography (RUS), which measures the natural resonance frequencies of a rock sample induced by an ultrasonic frequency sweep in the sample. These resonance frequencies are then numerically modelled to determine the bulk modulus and shear modulus of the rock sample.

Both of these methods use apparatus, developed by the authors, which clamp a cylindrical rock core sample between two sets of ultrasonic transducers. One set of transducer produces compressive ultrasonic waves, and the other produce shear ultrasonic waves. An analog-to-digital converter is used to read the changing voltage levels in the transducers, induced by the ultrasonic pulse travelling through the sample or the resonant vibrations of the sample induced by the ultrasonic frequency sweep in the sample.

Once the elastic parameters are known, they are applied to equations which relate specific storativity to the sample's elastic parameters. The storativity

values can then be calculated. The results obtained for the different core samples are shown in Tables E1 to E4.

**Table E1 - Time-of-flight results**

| Rock Type | Specific Storativity | Shear Velocity | Compressional Velocity |
|---|---|---|---|
| | 1/L | m/s | m/s |
| **TMG Sandstone** | 1.295E-06 | 1936 | 4879 |
| **Schist** | 6.459E-06 | 1617 | 2163 |
| **Quartzite** | 1.318E-06 | 2331 | 4806 |
| **Gneiss** | 1.048E-06 | 2590 | 7445 |
| **Shale (Campus site)** | 1.244E-05 | 1090 | 1559 |
| **Granite** | 1.786E-06 | 2409 | 4107 |
| **Dolerite** | 1.408E-06 | 2631 | 4773 |
| **Dolomite** | 1.148E-06 | 2881 | 6262 |
| **Sandstone (Campus site)** | 2.009E-05 | 1643 | 2011 |

**Table E2 - Resonant ultrasound spectrography results**

| Rock Type | Calculated Resonance Frequency | Recorded Resonance Frequency |
|---|---|---|
| | Hz | Hz |
| **TMG Sandstone** | 94 | 95 |
| **Schist** | 194 | 190 |
| **Quartzite** | 205 | 202 |
| **Gneiss** | 135 | 130 |
| **Shale (Campus site)** | 117 | 120 |
| **Granite** | 426 | 430 |
| **Dolerite** | 197 | 200 |
| **Dolomite** | 236 | 237 |
| **Sandstone (Campus site)** | 246 | 250 |

**Table E3 - Elastic parameter results**

| Rock Type | Shear Modulus | Bulk Modulus | Compressibility | Lamé Variable μ |
|---|---|---|---|---|
| | $Kg/s^2m$ | $Kg/s^2m$ | Pa | |
| **TMG Sandstone** | 4.952E+09 | 2.485E+10 | 4.025E-11 | 4.952E+09 |
| **Schist** | 3.862E+09 | 1.761E+09 | 5.678E-10 | 3.862E+09 |
| **Quartzite** | 8.034E+09 | 2.344E+10 | 4.266E-11 | 8.034E+09 |
| **Gneiss** | 9.573E+09 | 6.633E+10 | 1.508E-11 | 9.573E+09 |
| **Shale (Campus site)** | 1.480E+09 | 1.054E+09 | 9.488E-10 | 1.480E+09 |
| **Granite** | 7.027E+09 | 1.106E+10 | 9.046E-11 | 7.027E+09 |
| **Dolerite** | 9.858E+09 | 1.930E+10 | 5.181E-11 | 9.858E+09 |
| **Dolomite** | 1.167E+10 | 3.958E+10 | 2.527E-11 | 1.167E+10 |
| **Sandstone (Campus site)** | 3.248E+09 | 5.352E+08 | 1.868E-09 | 3.248E+09 |

**Table E4 - Additional parameter results**

| Rock Type | Lamé Variable λ | Young's Modulus | Poisson's Ratio | Acoustic Impedance |
|---|---|---|---|---|
| | | Pa | | |
| **TMG Sandstone** | 2.155E+10 | 1.393E+10 | 4.485E-01 | 3.283E+13 |
| **Schist** | 8.136E+08 | 6.694E+09 | 3.640E-01 | 2.602E+12 |
| **Quartzite** | 1.808E+10 | 2.163E+10 | 4.091E-01 | 3.465E+13 |
| **Gneiss** | 5.995E+10 | 2.740E+10 | 4.630E-01 | 9.466E+13 |
| **Shale (Campus site)** | 6.759E+07 | 3.024E+09 | 4.186E-02 | 1.312E+12 |
| **Granite** | 6.370E+09 | 1.740E+10 | 3.223E-01 | 1.339E+13 |
| **Dolerite** | 1.273E+10 | 2.527E+10 | 3.604E-01 | 2.749E+13 |
| **Dolomite** | 3.179E+10 | 3.188E+10 | 4.225E-01 | 5.565E+13 |
| **Sandstone (Campus site)** | 1.630E+09 | 3.223E+09 | 1.341E+02 | 6.439E+11 |

Although the study shows that specific storativity can be accurately determined by this system, it is important to realise that this system is also dependant on a number of things. The first is that the samples used in the testing process must be prepared very carefully. Attention to the cutting edge is essential, the flatter the cut, the better the result. The samples must also be selected to be as homogeneous as possible to avoid discrepancies between the time-of-flight and RUS results. The length of the sample must also be kept as long as possible to improve the sampling error induced. Although the system gives very good results due to the dual checking of time-of-flight and RUS methods results, it is always a good idea to check to results against average known specific storativity values for the rock type under test to determine a final result. This will give the user an idea of whether the results obtained are realistic or not, and may necessitate the need to test the sample again or use a different sample to compare the obtained values. Testing should be carried out in a noise-free environment to ensure that the results are not false and that all results should be checked at least twice to verify consistency.

# Acknowledgements

Thanks are given to Professors Botha and Cloot of the University of the Free State for their contributions to this study. The Water Research Commission is also thanked for funding this project.

# Table of Contents

# List of Figures



# List of Tables

# Chapter 1- Introduction

## *1.1 Background*

As groundwater becomes ever more important as a viable source of fresh water in arid and/or remote areas where surface water supplies are insufficient to sustain life, agriculture and industry, it has become important to accurately estimate, manage and monitor this valuable resource. Much has been done to improve the management of this valuable resource by the development of numerical models that give a realistic estimate on how groundwater reserves will react to changing circumstances in groundwater conditions. The accuracy of these predictions is limited to the effective accuracy of the predictive model, which in turn relies on accurate data on all the variables which will affect the flow of groundwater.

Storativity is one of the hydrological parameters which affect the flow of groundwater and the outcome of predictive models. Storativity is an ambiguous parameter in that it is dependent on two unknown variables, namely aquifer thickness and rock elastic parameters. At present, storativity is estimated using borehole pump test data and inverse modelling, which is not always an accurate measure of the parameter.

## *1.2 Objectives*

This paper presents a method developed by the authors to determine storativity by determining actual specific storativity values of the rock that make up an aquifer.

## *1.3 Methodology*

Specific storativity is the parameter which specifies the amount of water released by a rock sample when exposed to a change in pressure head, as is the case when a confined aquifer is mined. Specific storativity is determined by experimentally measuring the elastic parameters of a rock sample, in this case a core sample. These measurements are done in two ways. The first is to measure the compressive and shear wave velocities of the rock by inducing an ultrasonic pulse into the one side of the sample core and measuring the time it takes the pulse to travel through the sample. The travel times are then converted into compressive and shear velocities which in turn are used to determine the bulk modulus and shear modulus of the sample. The second method is to use resonant ultrasound spectrography (RUS) which measures the natural resonance frequencies of a rock sample induced by an ultrasonic frequency sweep in the sample. These resonance frequencies are then

numerically modelled to determine the bulk modulus and shear modulus of the rock sample.

Both of these methods use apparatus, developed by the authors, which clamp a cylindrical rock core sample between two sets of ultrasonic transducers. One set of transducers produce compressive ultrasonic waves and the other produce shear ultrasonic waves. An analog to digital converter is used to read the changing voltage levels in the transducers, induced by the ultrasonic pulse travelling through the sample or the resonant vibrations of the sample induced by the ultrasonic frequency sweep in the sample. Once the elastic parameters of the rock samples are known, they are applied to equations which relate specific storativity to the elastic parameters of the samples. The resultant storativity value can then be determined.

## *1.4 Theory of Ultrasound*

Before the RUS and time-of-flight technique's can be discussed, a proper basic understanding of ultrasound acoustics must be formed. This section will discuss the basics of ultrasound acoustics and wave travel in elastic media.

### 1.4.1 What is ultrasound

Sound generated above the human hearing range (typically 20 KHz) is called ultrasound. However, the frequency range normally employed in ultrasonic resonance testing and s-value determinations is 1 KHz to 1 MHz. Although ultrasound behaves in a similar manner to audible sound, it has a much shorter wavelength. This means it can be reflected off very small surfaces such as defects inside materials. It is this property that makes ultrasound useful for non-destructive testing of materials. The Acoustic Spectrum in Figure 1 breaks down sound into 3 ranges of frequencies. The Ultrasonic Range is then broken down further into 3 sub sections (Wayne et al., 2005).

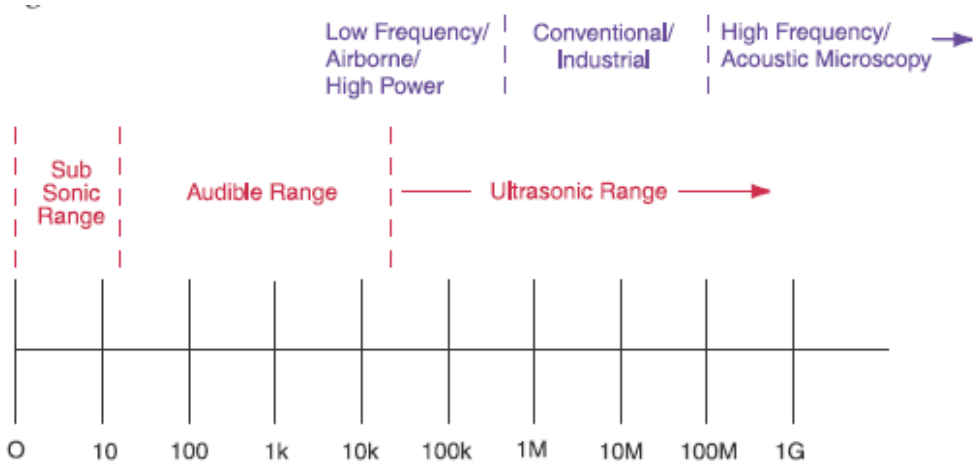


**Figure 1 - Audio frequency range**

### 1.4.2 Frequency, period and wavelength

Ultrasonic vibrations travel in the form of a wave, similar to the way light travels. However, unlike light waves, which can travel in a vacuum (empty space); ultrasound requires an elastic medium such as a liquid or a solid. Shown in Figure 2 are the basic parameters of a continuous wave (cw). These parameters include the wavelength (λ) and the period (T) of a complete cycle.

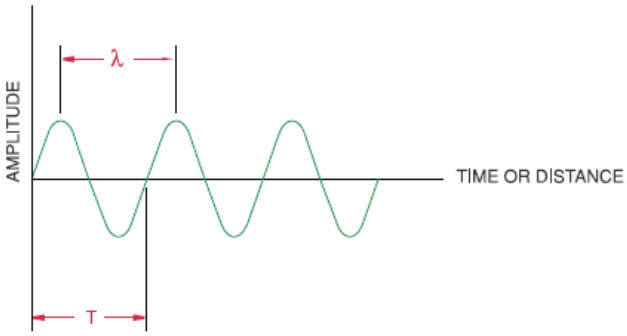


**Figure 2 - Waveform**

The number of cycles completed in one second is called frequency (f) and is measured in Hertz (Hz), some examples follow (Powis et al., 1998):

- 1 cycle/second= 1Hz
- 1000 cycles/second= 1KHz
- 1,000,000 cycles/second= 1MHz

The time required to complete a full cycle is the period (T), measured in seconds. The relation between frequency and period in a continuous wave is given in equation 1.

$$f = \frac{1}{T}$$

**Equation 1**

### 1.4.3 Velocity of ultrasound and wavelength

The velocity of ultrasound (c) in a perfectly elastic material at a given temperature and pressure is constant (Wayne et al., 2005). The relation between c, f, λ and T is given by Equations 2 and 3:

$$\lambda = \frac{c}{f}$$

**Equation 2**

$$\lambda = cT$$

**Equation 3**

λ = Wavelength
c = Material Sound Velocity
f = Frequency
T = Period of time

### 1.4.4 Wave propagation and particle motion

The most common methods of ultrasonic examination utilize either longitudinal waves or shear waves. Other forms of sound propagation exist, including surface waves and Lamb waves.

The longitudinal wave is a compressional wave in which the particle motion is in the same direction as the propagation of the wave.

The shear wave is a wave motion in which the particle motion is perpendicular to the direction of the propagation.

Surface (Rayleigh) waves have an elliptical particle motion and travel across the surface of a material. Their velocity is approximately 90% of the shear wave velocity of the material and their depth of penetration is approximately equal to one wavelength.

Plate (Lamb) waves have a complex vibration occurring in materials where thickness is less than the wavelength of ultrasound introduced into it.

Figure 3 provides an illustration of the particle motion versus the direction of wave propagation for longitudinal waves and shear waves (Wayne et al., 2005).

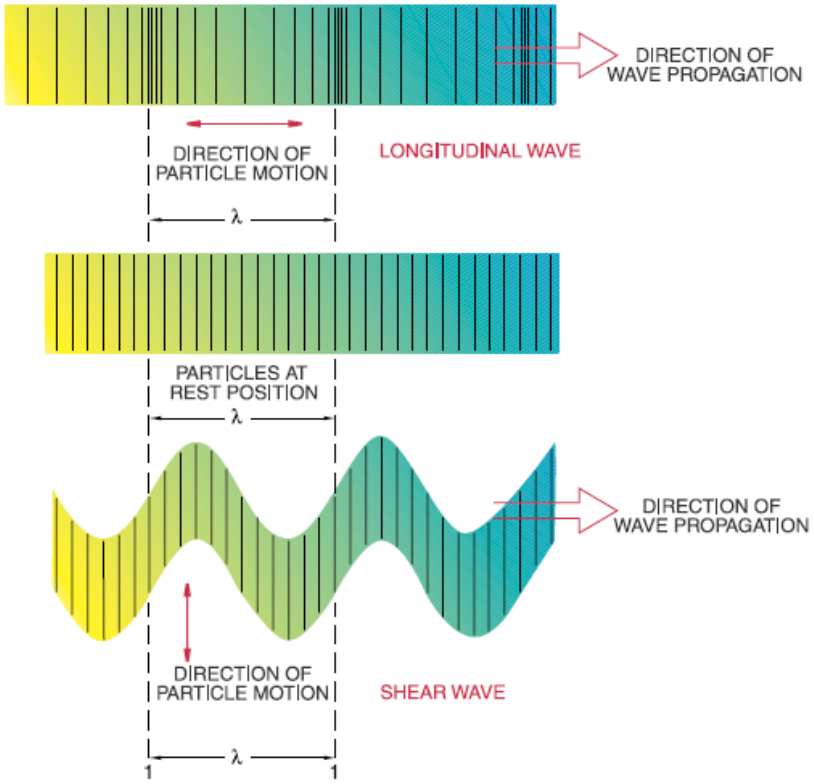


**Figure 3 - Longitudinal versus shear waves**

### 1.4.5 Applying ultrasound

Ultrasonic non-destructive testing introduces high frequency sound waves into a test object to obtain information about the object without altering or damaging it in any way. Two basic quantities are measured in ultrasonic testing; they are time-of-flight or the amount of time for the sound to travel through the sample and amplitude of received signal. Based on velocity and round trip time-of-flight through the material the material thickness can be calculated as follows:

$$T = \frac{cts}{2}$$

**Equation 4**

*T* = Material Thickness
c = Material Sound Velocity
ts= Time-of-flight

Measurements of the relative change in signal amplitude can be used in determining the resonance frequencies of a material. The relative change in signal amplitude is commonly measured in decibels. Decibel values are the logarithmic value of the ratio of two signal amplitudes. This can be calculated using the following equation (Jennings and Flint, 1995):

$$dB = 20\log 10\left(\frac{A1}{A2}\right)$$

**Equation 5**

dB = Decibels
A1 = Amplitude of signal 1
A2 = Amplitude of signal 2

### 1.4.6 Sensitivity and resolution

Sensitivity is the ability of an ultrasonic system to detect reflectors (or impurities) at a given depth in a test material. The greater the signal that is received from these reflectors, the more sensitive the transducer system.

Axial resolution is the ability of an ultrasonic system to produce simultaneous and distinct indications from reflectors located at nearly the same position with respect to the sound beam.

Near surface resolution is the ability of the ultrasonic system to detect reflectors located close to the surface of the sample (Jennings and Flint, 1995).

### 1.4.7 Transducer waveform and spectrum

Transducer waveform and spectrum analysis is done according to test conditions and definitions of ASTM E1065. Typical units are MHz for frequency analysis, microseconds for waveform analysis, and dB down from peak amplitude. Figure 6 illustrates waveform duration at the -14 dB level or 20% amplitude of peak. The -40 dB waveform duration corresponds to 1% amplitude of peak. Figure 5 illustrates peak frequency, upper and lower -6dB frequencies and MHz bandwidth measurements. The relation between bandwidth and waveform duration is shown in Figure 6. The scatter is wider at -40 dB because the 1% trailing end of the waveform contains very little energy and so has very little effect on the analysis of bandwidth. Because of the scatter it is most appropriate to specify waveforms in the time domain (microseconds) and spectrums in the frequency domain (Wayne et al., 2005).

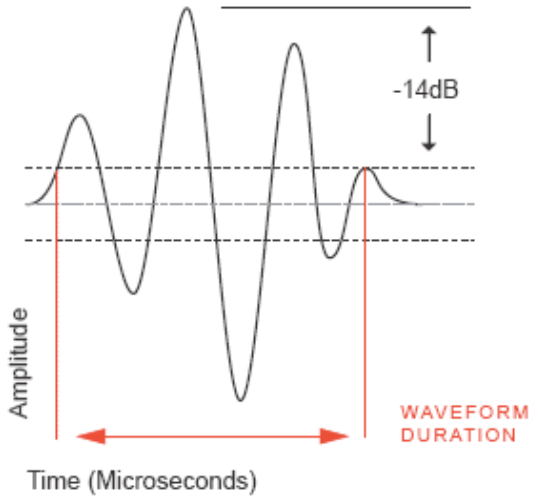


**Figure 4 - Ultrasound pulse**

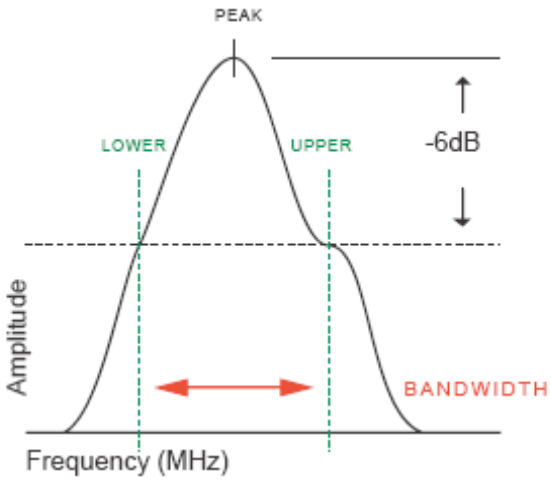


**Figure 5 - Waveform spectrum**

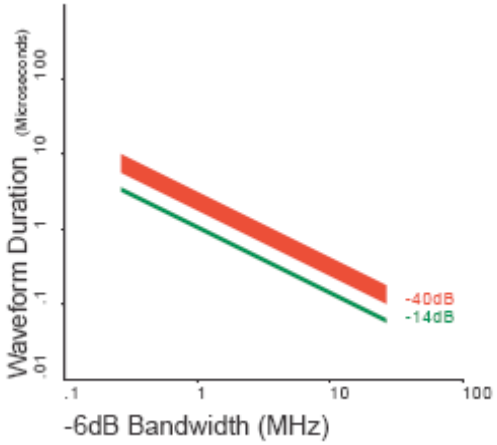


**Figure 6 - Waveform duration to bandwidth**

### 1.4.8 Acoustic impedance, reflectivity, and attenuation

The acoustic impedance of a material is the opposition to displacement of its particles by sound and occurs in many equations. Acoustic impedance is calculated as follows:

$$Z = \lambda c$$

**Equation 6**

Z = Acoustic Impedance
c = Material Sound Velocity
λ = Material Density

The boundary between two materials of different acoustic impedances is called an acoustic interface. When sound strikes an acoustic interface at normal incidence, some amount of sound energy is reflected and some amount is transmitted across the boundary.

The dB loss of energy on transmitting a signal from medium 1 into medium 2 is given by (Wayne et al., 2005):

$$dB = 10\log 10\left(\frac{4Z1Z2}{2(Z1+Z2)}\right)$$

**Equation 7**

Z1 = Acoustic Impedance of First Material
Z2 = Acoustic Impedance of Second Material

The dB loss of energy of the echo signal in medium 1 reflecting from an interface boundary with medium 2 is given by:

$$dB = 10\log 10\left(\frac{2(Z2-Z1)}{2(Z1+Z2)}\right)$$

**Equation 8**

# Chapter 2 - Theory of Time-of-flight

## *2.1 Introduction*

Time-of-flight methods have been used for many years as a method to determine sound velocity variables for a variety of materials. Its most common application is in the building industry where two way time-of-flight systems are used to determine building material strength. An unfortunate disadvantage of two way time-of-flight systems available today is that they must make use of high frequency ultrasonics to avoid the dimensional constraints of the material being tested; associated with reflections off boundaries that interfere with the propagation of the ultrasound traveling through the sample. The wavelength of the ultrasound used must be much smaller than the dimensions of the sample under test in order to deliver accurate results.

The main problem with the use of high frequency ultrasound in a solid is that it is quickly attenuated by absorption and scattering in the sample, thus affecting its effective range. Te resolution of the time-of-flight method is improved by increased sample length; this is a major restriction in terms of sample size that can be used practically.

In the time-of-flight system used in this study, only one way travel is used. This eliminates the need to use high frequency ultrasonics and allows for longer sample lengths to be used, without ill effects (Choudhari et al., 2002).

## *2.2 Methodology*

The time-of-flight method measures the time it takes a sound pulse of a given frequency to travel through a substance, in this case a cylindrical core rock sample, from a transmitting ultrasound transducer, to a receiving ultrasound transducer at the opposite end of the sample. This is achieved by clamping piezo-electric transducers to either end of the cylinder rock sample and inducing a pulse of ultrasound at one transducer. The receiving ultrasound transducer is then simultaneously recorded by means of analog-to-digital converters at a rate of one million samples per second. The time it takes for the ultrasound pulse to travel across the sample is measured by looking at the recorded data and pinpointing a sudden rise in voltage at the frequency of the traveling ultrasonic pulse. The time is then recorded at this point and is divided into the length of the sample. This gives a value for the velocity of the wave for that specific sample.

The samples used in determination of time-of-flight methods are fresh samples taken from water saturated core samples. This simulates actual seismic velocities that would occur underground and gives the most realistic results on elastic parameters (Choudhari et al., 2002).

## *2.3 Modes of Travel*

Figure 7 shows all the modes of travel a compressional or shear wave can induce in a cylindrical core sample. The transducers used in this study make use of only compressional mode 18 and shear mode 9. These compressional and shear velocities define the elastic parameters of the sample (Leisure and Willis, 1997).

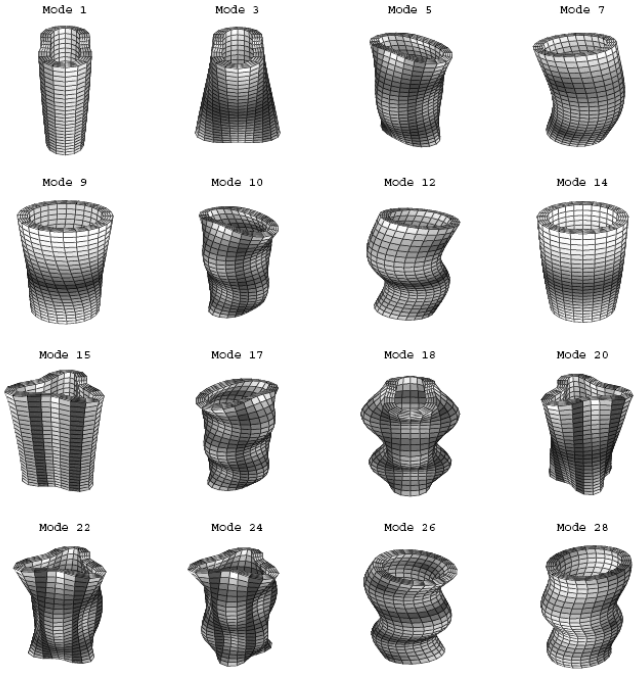


**Figure 7- Modes of vibration**

## *2.4 Velocity Calculation and Assumptions and Limitations*

An inherent measure of uncertainty is always present in time-of-flight calculations. This is due to the digital sampling limitations placed on the system by hardware constraints in the speed a voltage can be sampled. In the case of this system, the voltage produced by the receiving piezo transducer is sampled discretely every 1 micro second. This means the system can sample at a rate of one million samples per second. Even though this sounds like an extremely fast sample rate, there is still a small error or uncertainty in the actual velocity, to the measured velocity. The discrete nature of digital sampling produces this error by allowing a small pause between samples. If the pulse arrives at the receiver in between these samples there is an uncertainty as to the exact time the pulse arrived. The faster the sampling rate the smaller the error. However, modern high frequency sampling devices are very expensive and are usually not cost effective to implement. There are fortunately other ways to improve the error in standard systems by implementing the use of longer rock samples. The longer the rock sample, the more accurate a velocity will be measured in the sample. Practically, it is not

possible to use core samples that are too long as it is rare that samples are not broken during the drilling process. This study has made use of samples ranging from eight to thirty centimeters in length. This is mainly due to the fact that most of the raw core samples are only found in lengths in this range. Another contributing factor to velocity uncertainty is sample velocity. The higher the velocity for a given sample length the higher the error of the measurement will be. This is a non-linear function and becomes exponentially bigger as the sample velocity increases (Madeira et al., 1999).

## *2.5 Calculation of Elastic Parameters*

In time-of-flight methods, elastic parameters are calculated using the sample velocity measurements for compressional waves and shear waves of a sample. To calculate shear modulus the equation below is used (Boyd, 2003).

$$G = V_s^2 \times \rho$$

**Equation 9**

G = Shear modulus
Vs = Shear velocity
p = Density of the rock sample

Using the shear modulus G, we can then determine the bulk modulus of the sample using the equation:

$$K = V_p^2 \rho - \frac{4G}{3}$$

**Equation 10**

K = Bulk modulus
Vp = Compressional wave velocity
G = Shear modulus
p = Density of the rock sample

Together the bulk modulus and the shear modulus describe the elastic parameters of the rock sample (Boyd, 2003).

## *2.6 Benefits and Disadvantages*

Time-of-flight methods benefit in that they are simple to implement. Reliable and consistent measurements are obtained using this method. Disadvantages included uncertainties associated with sample rates which produce predictable errors in the seismic velocities measured using the method.

# Chapter 3 - Theory of Resonant Ultrasound Spectrography

## *3.1 Introduction*

Resonant ultrasound spectrography (RUS) is a method that makes use of the natural resonance frequencies of an object of known dimensions to determine the elastic parameters of that object. RUS methods are useful in that they give an average value for elastic parameters for a test object being measured. This gives a far better estimate for specific storativity values, in samples that are very large or very heterogeneous, than time-of-flight methods which tend to have lower specific storativity estimates. This is due to the fact that it finds the maximum velocities in the sample rather than the average. This problem is averted in smaller samples as heterogeneities are minimized in the sample.

The samples used in determination of RUS methods are fresh samples taken from water saturated core samples. This simulates actual elastic parameters that would occur underground and gives the most realistic results (Zadler et al., 2003).

## *3.2 Modes of Vibration*

To better understand RUS methods, a basic understanding of the fundamental modes of distortion for an object must be understood. Since this study uses core drilling samples of cylindrical shape, only cylinders will be discussed.

All modes of distortion in a sample can be put into three classes or class modes. These are (Zadler et al., 2004):

- Flexural modes that are produced by acoustic energy travelling down the sample at an angle other than that of the axis (Figure 8).

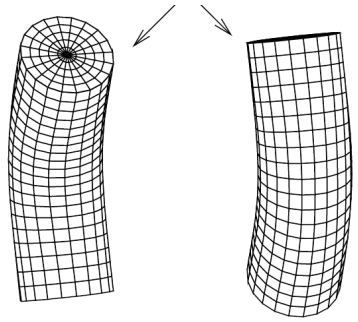

**Figure 8 - Flexural class mode (Zadler et al., 2004).**

- Torsional modes that are caused by shear waves passing though the sample and cause a twisting motion on the sample when resonance of the sample occurs (Figure 9).

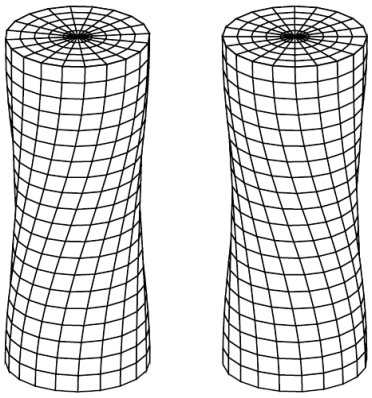

**Figure 9 - Torsional class mode (Zadler et al., 2004).**

- The extensional mode is a mixture of compressional and shear waves, which causes the sample to compress laterally with low frequency acoustic waves (Figure 10).

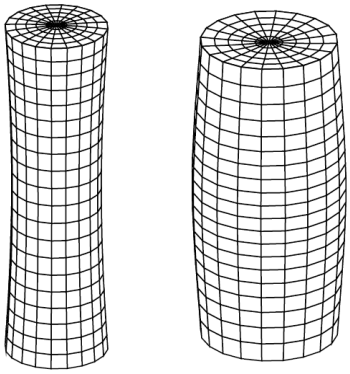

**Figure 10 - Extensional class mode (Zadler et al., 2004).**

All of these modes may appear in a RUS measurement. The measurement equipment detects these resonant frequencies of all class modes then uses these frequencies to determine the elastic parameters of the sample.

## *3.3 Methodology*

In order to determine the elastic parameters of the sample, which is required to determine an S-value for the sample, the frequency spectrum of the test sample is needed to be input into a forward model. The model used in this experiment is the Breit-Wigner model, and takes as its inputs, the actual resonance spectrum data of the tested sample. The model then fits the data to a set of parameters by using iterative methods. The results of this fitting process, is a set of curves that replicate the shape and amplitude of the actual resonance frequency peaks produced by the tested sample. These fitting curves have peaks as well, which are analyzed by the model to give the output in the form of frequency and Q-values of these fitted peaks. Values like GAMMA which where used by the model to determine the iterative fit of the output curves are also available as an output.

Once the fitting parameters are determined, this data, i.e. the frequency and Q-values of the forward model, is used to calculate either the sample dimensions or the elastic moduli of the sample. This is done by using an inversion model. Since the dimensions of the sample are known already, this is used as an input to the inversion model for the calculation of the elastic moduli of the sample (Zadler and Le Rousseau, 2003).

## *3.4 Calculation of Elastic Parameters by Numerical Methods*

Since there are no general analytical solutions to solving three dimensional RUS elastic parameters, a numerical approach must be implemented. To implement the forward model a program called Fitspectra is used. Fitspectra makes use of the Breit-Wigner model to fit the modelled data to the actual frequency data recorded. A complete mathematical description of this model is given in a paper by Zadler and Le Rousseau (2003).

A frequency sweep is generated by an audio processing program attached to a computer sound card. Figure 11 shows the frequency sweep setup window. The resonant frequency data is then recorded by the computer audio recording device. A test frequency sweep recording is shown in Figure 12. This sweep shows distinct amplitude increases at various frequencies.

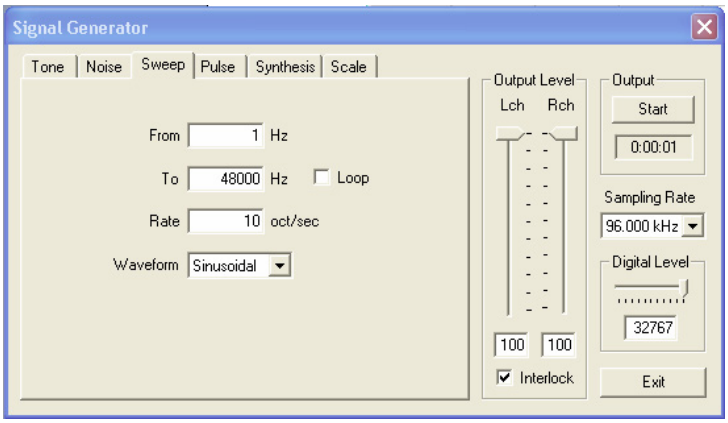


**Figure 11 - Audio sweep setup**

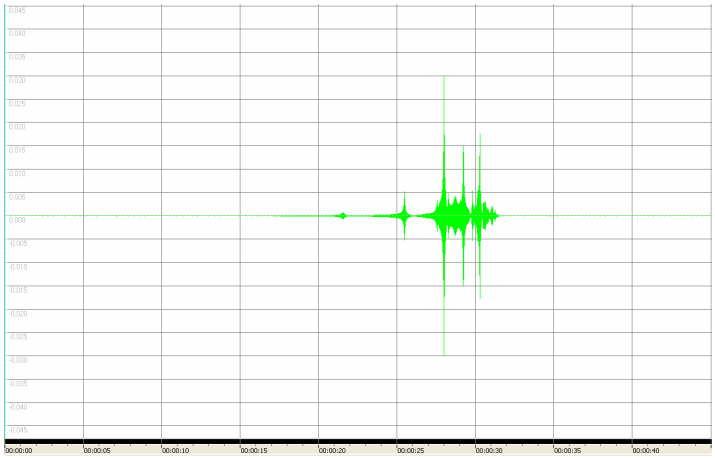

**Figure 12 - Recorded waveform**

This recorded sweep data is imported into Fitspectra as shown on Figure 13

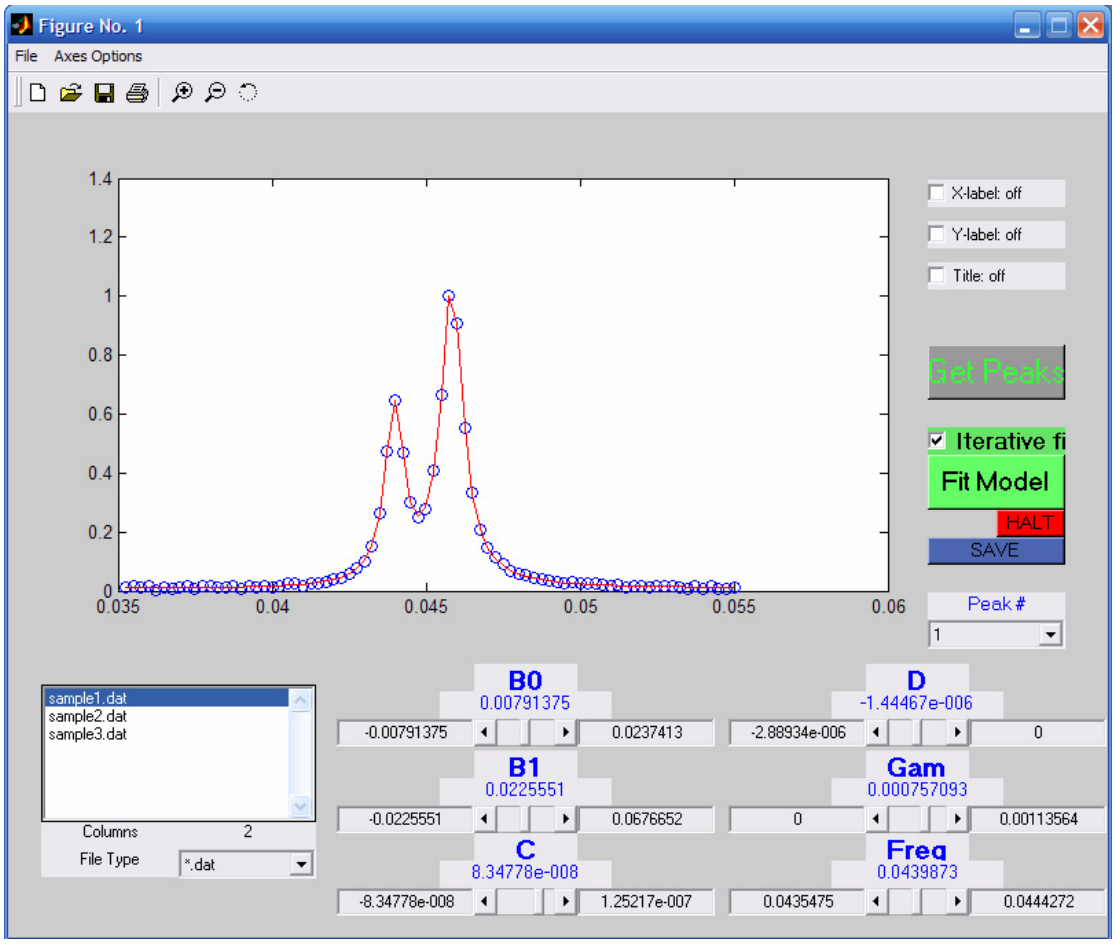


**Figure 13 - Fitspectra curve fitting**

Fitspectra applies a forward model to the frequency sweep data to generate a fitting curve which is used to generate a table of resonant frequency sweeps and corresponding Q-values for those resonant frequencies.

These frequency and Q-values are then used by a pre-conjugate gradient forward model, called the COOOL model, to calculate its normal modes of resonance. An inverse model is then used to determine the elastic properties of the sample (Zadler and Le Rousseau, 2003).

## *3.5 Alternative Approach by Analytical Methods*

An alternative method can be used to calculate shear modulus by means of analytical methods. The analytical method makes use of physical constraints on the dimensions of the sample to allow the calculation of the lowest torsional mode of resonance. In the event that a sample with diameter equal to length is used in RUS, then the lowest or first resonant frequency is the fundamental torsional mode of resonance.

Once this frequency is known the following equation can be used to calculate the shear modulus of the sample by analytical means.

$$f = \frac{n}{2L}\sqrt{\frac{G}{\rho}}$$

**Equation 11**

f = Resonant Torsional mode frequency
n = 1 for lowest natural frequency
L = Length of the sample
G = Shear modulus
ρ = Density of the rock sample

The use of this method gives the user the ability to apply a far more accurate and simpler method to compare the results of time-of-flight methods to that of RUS methods. It allows a simple analytical approach and negates the need to use numerical methods to check RUS results. This study uses this approach to determine if the elastic parameters determined for a sample by time-of-flight methods are correct, by comparing the calculated frequency spectrum using the time-of-flight data to the actual RUS frequency spectrum recorded from the sample. If the calculated and measured frequency spectrum line up, then the results are accurate. If not, then the measurements must be taken again with different samples (Wang and Lakes, 2003).

The use of this method takes the best advantage of both RUS and time-of-flight methods and makes efficient use of computer processing power by minimizing the necessary computation time.

## *3.6 Advantages and Disadvantages*

RUS methods are an effective means for deriving elastic parameters of an object in that they provide an average for the elastic parameters of all the inhomogeneities in the sample. This is however a computational intensive exercise and needs very well cut samples to be achieved. However, by using the analytical computation method instead of the numerical method, these disadvantages can be avoided.

# Chapter 4 - Theory of Specific Storativity

## *4.1 Introduction*

The specific storativity is the amount of water which a given volume of aquifer will produce, provided a unit change in hydraulic head is applied to it (while it still remains fully saturated); it has units of inverse length, [$L^{-1}$]. It is the primary mechanism for storage in confined aquifers. It can be expressed as the volume of water released from storage per unit decline in hydraulic head in the aquifer, per unit volume of aquifer. It is defined by the equation:

$$S_s = \frac{Vw}{\frac{dH}{Va}}$$

**Equation 12**

Ss = Specific storativity
Vw = Volume of water in the aquifer
dH = Change in head in the aquifer
Va = Volume of the aquifer

In terms of measurable physical properties, specific storativity can be expressed as:

$$S_s = \rho g(\alpha + \eta\beta)$$

**Equation 13**

ρ = density of water
g = gravitational constant
*α* = compressibility of the rock
β = compressibility of the water
η = porosity of the rock

An interesting indication this equation has, is that since the compressibility of water is very small, the sample porosity will have a very small influence on the specific storativity of the sample. The largest contributor to the specific storativity of a sample is the compressibility of the sample. This is determined by the bulk modulus of the sample (Hermance, 2003). The compressibility of the rock matrix is given by the equation:

$$\alpha = \frac{1}{K}$$

**Equation 14**

K = Bulk modulus of the rock sample

The compressibility of water is taken as a constant. Storativity is the vertically averaged specific storativity value for an aquifer or aquitard. For a homogeneous aquifer or aquitard they are simply related by

$$S = Ss \times b$$

**Equation 15**

*b* = thickness of aquifer.

Storativity is a dimensionless quantity, and can be expressed as the volume of water released from storage per unit decline in hydraulic head in the aquifer, per unit area of the aquifer. This is defined by the following equation:

$$S = \frac{dVw}{dH \times A}$$

**Equation 16**

dVw = change in volume of water
dH = change in head
A = area

## *4.2 Concepts*

Figure 14 shows the conceptual diagram of how specific storativity is defined in a confined aquifer. It can be expressed as the volume of water released from storativity per unit decline in hydraulic head in the aquifer, per unit volume of aquifer. It is important to note that this applies only to confined aquifers that are fully saturated. Once the aquifer is no longer fully saturated the equations revert to an unconfined aquifer condition and specific yield is calculated (Hermance, 2003).

Figure 15 shows the storativity concept diagram. Storativity is related to specific storativity by the thickness of the aquifer [b] (Hermance, 2003). The thicker the aquifer, the larger the value of storativity will be.

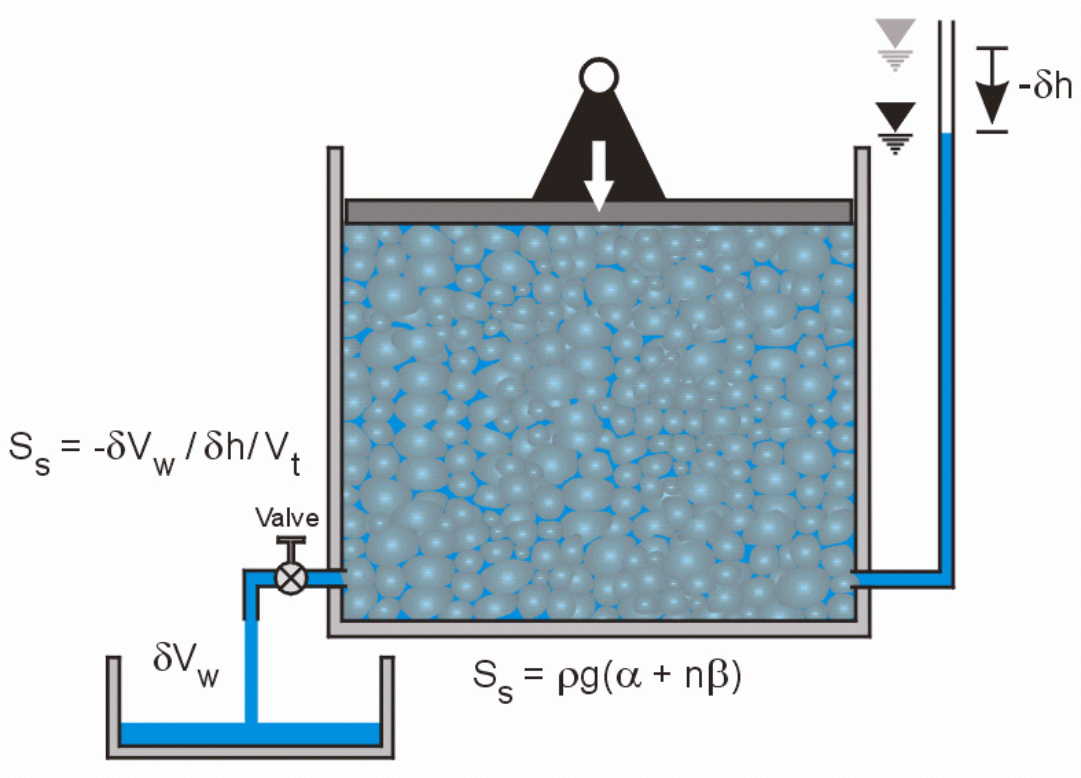


**Figure 14 - Specific storativity concept (Hermance, 2003).**

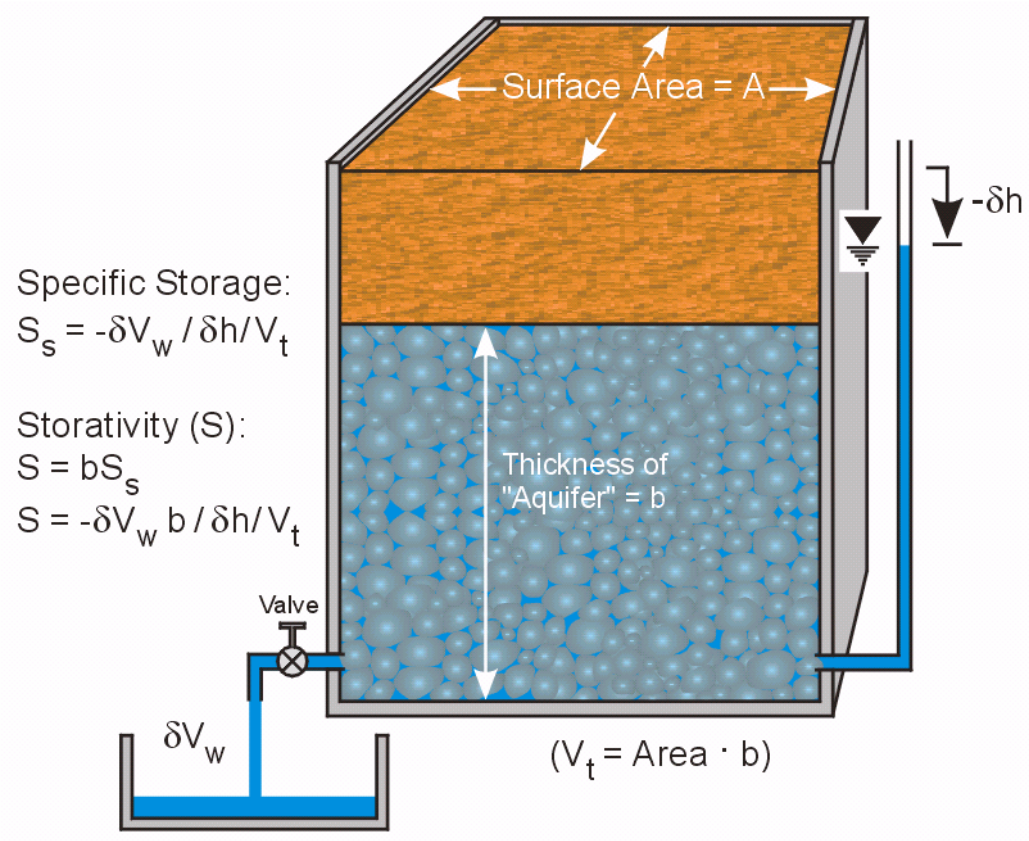


**Figure 15 - Storativity concept (Hermance, 2003).**

# Chapter 5 - Additional Calculated Parameters

## *5.1 Lamé's Constants*

The Lamé constants λ and μ can be calculated in a number of ways using a number of different elastic and physical rock properties. They define the stress to stain relations of a rock sample. The equations below show a few of these equations (Weisstein, 2007).

$$\lambda \equiv \frac{vE}{(1+v)(1-2v)}$$
$$\lambda = K - \frac{2}{3}G$$
$$\lambda = \frac{2vG}{1-2v}$$
$$\lambda = 3K\frac{v}{1+v}$$
$$\lambda = \rho(v_p^2 - 2v_s^2)$$

$$\mu \equiv \frac{E}{2(1+v)}$$
$$\mu = \frac{3}{2}(K - \lambda)$$
$$\mu = \lambda\frac{1-2v}{2v}$$
$$\mu = 3K\frac{1-2v}{2+2v}$$
$$\mu = \rho v_s^2$$

**Equation 17**

*E* = Young's modulus
v = Poisson ratio
*G* = shear modulus
*K* = bulk modulus
p = density
Vp = *P*-wave speed
Vs = *S*-wave speed

## *5.2 Young's Modulus*

Young's modulus *E* is defined as (Weisstein, 2007):

$$E \equiv \frac{Stress}{Strain}$$

**Equation 18**

Which is equal to:

$$E = \frac{\mu(3\lambda + 2\mu)}{\lambda + u}$$

**Equation 19**

Where μ and λ are Lamé constants (Weisstein, 2007).

## *5.3 Poisson's Ratio*

The Poisson ratio, v, can be described in terms of the Lamé constants $\lambda$ and μ as well as elastic parameters K and G and velocity values Vs and Vp (Weisstein, 2007).

$$v = \frac{\lambda}{2(\lambda + \mu)}$$
$$v = \frac{\lambda}{2K - \lambda}$$
$$v = \frac{3K - 2\mu}{2(3K + \mu)}$$
$$v = \frac{1}{2}\frac{(\frac{V_p}{V_s})^2 - 2}{(\frac{V_p}{V_s})^2 - 1}$$

**Equation 20**

$\lambda$ = Lamé constant
μ = Lamé constant
*K* = bulk modulus
U = rigidity
Vp = *P*-wave speed
Vs = *S*-wave speed

# Chapter 6 - Experimental Apparatus

## *6.1 Introduction*

Experimental apparatus had to be developed by the authors in order to evaluate the elastic parameter of rock test samples. A basic clamping system was used to fix the samples firmly against the ultrasonic transducers in order to make a good acoustic coupling. The clamping system is designed to accommodate 40 cm long samples, allowing for very accurate readings of shear and compressional velocities, but also allowing for a variable sample length for operating flexibility. The software developed for the system allows the user to make use of samples of varied dimensions by making provision for custom dimensions to be input into the calculations for specific storativity. An added feature of the clamping system is that the compressional and shear transducers can be interchanged on the same system, dispensing the need to have two separate clamps for each. The first problem to address when taking velocity measurements in a core sample is to prepare the sample in the correct manner. The next section deals with sample preparation.

## *6.2 Sample Preparation*

For this project, twelve samples were used to evaluate the system. These samples were gathered from varying geologies of known hydrological parameters. The samples were of different lengths and diameters as well as shape, that being, cylindrical or half cylinders. This large variation in sizes and shapes of the samples gives a good platform on which to test the systems performance (Zadler and Le Rousseau, 2003). Figures 16 and 17 show the samples used in the testing of the system.


**Figure 16 - Test Samples**

**Figure 17 - Half cylinder sample shapes**

The most important part in preparing a sample is to make sure the sample core has a perpendicular flat edge on either side of the core cylinder. This is achieved by using a cutting disk and core cutter. It is very important that the core sides be cut straight and flat. If this is not done, the acoustic coupling between the core and transducer will be poor and it will attenuate the acoustic wave drastically, making velocity measurements very difficult. Figure 18 shows an example of a core cutting with a very flat face.

**Figure 18 - Cut edge**

After the sample is cut its mass must be measured, preferably by an accurate lab scale. The sample should then be marked by name and its critical information written on the sample, such as, mass, length, diameter, and porosity. It is also necessary to indicate the measurement direction marked on the sample. This is done by indicating by an arrow in the direction from the transmitting transducer to the receiving transducer. This is done to ensure consistency should measurements be taken again. Figure 19 shows the markings made on the test samples.


**Figure 19 - Sample marking**

In the case of the compressional wave velocity measurements, glycerin should be used between the transmitting and receiving transducers to allow for the acoustic coupling and better signal penetration. Glycerin is used due to the fact that it has an acoustic impedance similar to rock and is easily washed of by water. Figure 20 shows how the glycerin is applied to the sample.

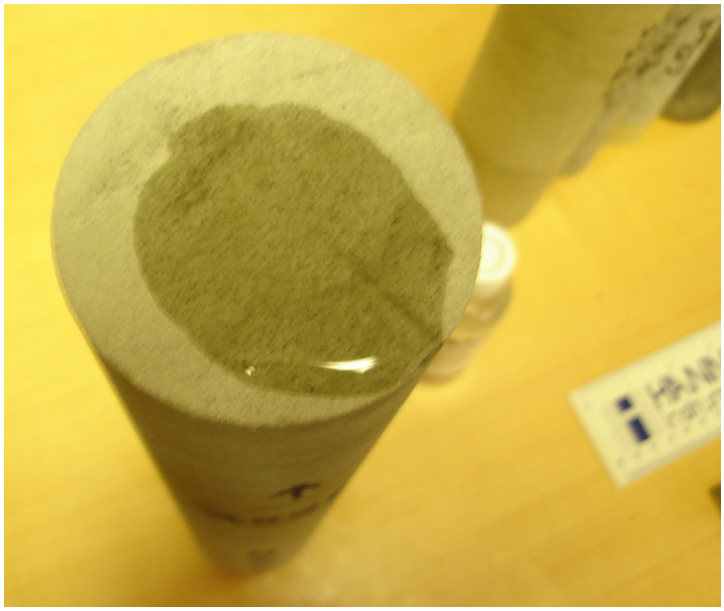

**Figure 20 - Glycerin as an acoustic contact agent**

Samples should be selected and cut according to the homogeneity of the sample. If there are severe inhomogeneities in a sample it should not be used as there will be inconsistencies between the time-of-flight and RUS evaluations of the elastic parameters. As mentioned in previous chapters, RUS measures the average elastic parameters of the conglomerate sample and time-of-flight measures the highest elastic parameter values of the

sample. Large sample inhomogeneities will cause large variations in the average elastic values to the highest elastic values for a given sample (Zadler and Le Rousseau, 2003).

## *6.3 Apparatus*

Figure 21 shows the apparatus developed for this study. The sample is clamped between the transducers as shown in Figure 22. The IOTech Personal DAQ system is used to produce the ultrasonic data to the transmitting transducer and record the data from the receiving transducer. The transducers are connected in a differential connection to the data acquisition tool. The DAQ sends the data to the software via USB cable Wang and lakes, 2003).

**Figure 21 - Experimental apparatus**

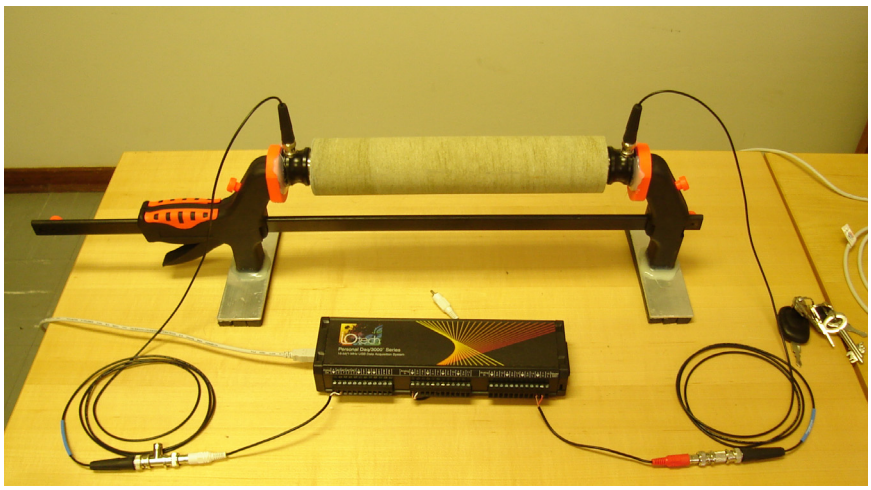

**Figure 22 - Clamped sample**

Figure 23 shows the transducer – sample coupling. The transducer is isolated from the clamp by a rubber cushion to which it is glued. This is essential as it will block most of the acoustic energy from traveling through the clamping mechanism to the receiving transducer.

**Figure 23 - Transducer fitting**

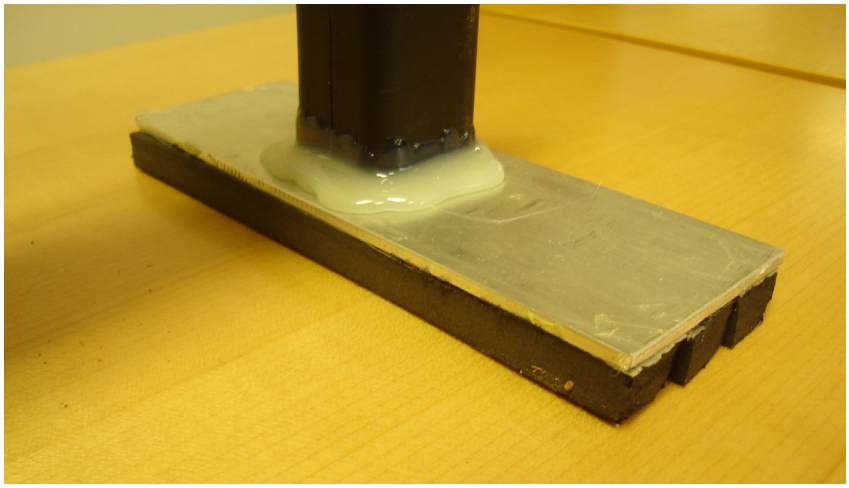

**Figure 24 - Isolation base**

The transducers used in the apparatus are manufactured by Panameterics. A pair of compression transducers is used as the transmitter and receiver in the compressional wave speed setup. A pair of shear wave transducers is used in the shear wave speed setup (Wang and Lakes, 2003).

The compressional wave transducers have a bandwidth of 1 MHz and resonate at 500 KHz. The shear transducers have a bandwidth of 500 KHz and resonate at 250 KHz.

Figures 25 and 26 show the shear and compressional wave transducers. Both sets are encased in a metal covering for durability. The shear wave transducer is physically larger than the compressional transducer; this limits the size of the samples to the maximum size in the shear configuration.

**Figure 25 - Shear wave transducer**

**Figure 26 - Compressional wave transducer**

Both the shear and compressional transducers are glued to the rubber base plates. This is done to minimize the acoustic coupling between the base plates and the transducers. The rubber base plates further attenuate acoustic coupling between the transducers and the apparatus. This drastically improves the signal to noise ratio on highly attenuated signals.

## *6.4 Software*

The software used to record the signals coming from the DAQ system to the computer is called DAQView and is provided with the IOTech Personal DAQ system. Since the software is a third party application it must be used separately from the analysis software developed for this project. The DAQView software provides a user friendly interface to set up the DAQ hardware and to provide a customizable file format that can store data in a way that other programs can access the data simply.

Figure 27 shown above illustrates the data destination window of the DAQ view software. Here the data file name and directory that it is stored in can be set or changed by the user. A default name “daqv.*” is used to name the recorded file. The data is stored in binary format, but is automatically converted to a text (txt) file by DAQView. This text file is used to interpret the data.

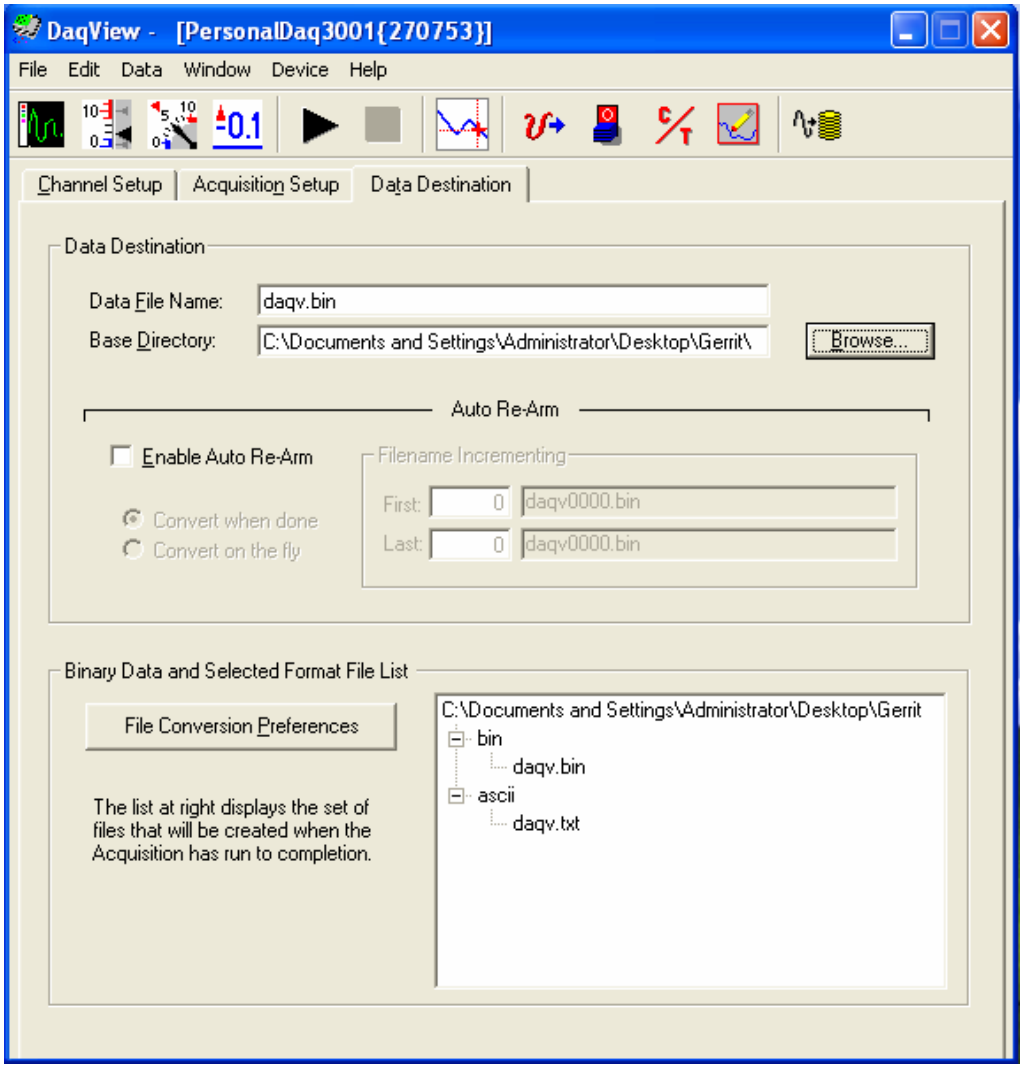


**Figure 27 - DAQ file system**

The DAQView Acquisition Setup window (Figure 28) is used to setup the hardware functions in order to take a reading. The hardware is setup to immediately start recording data when an ultrasound pulse is generated by the system. This allows the system to have a very accurate time count and thus give an exact time-of-flight for the sample.

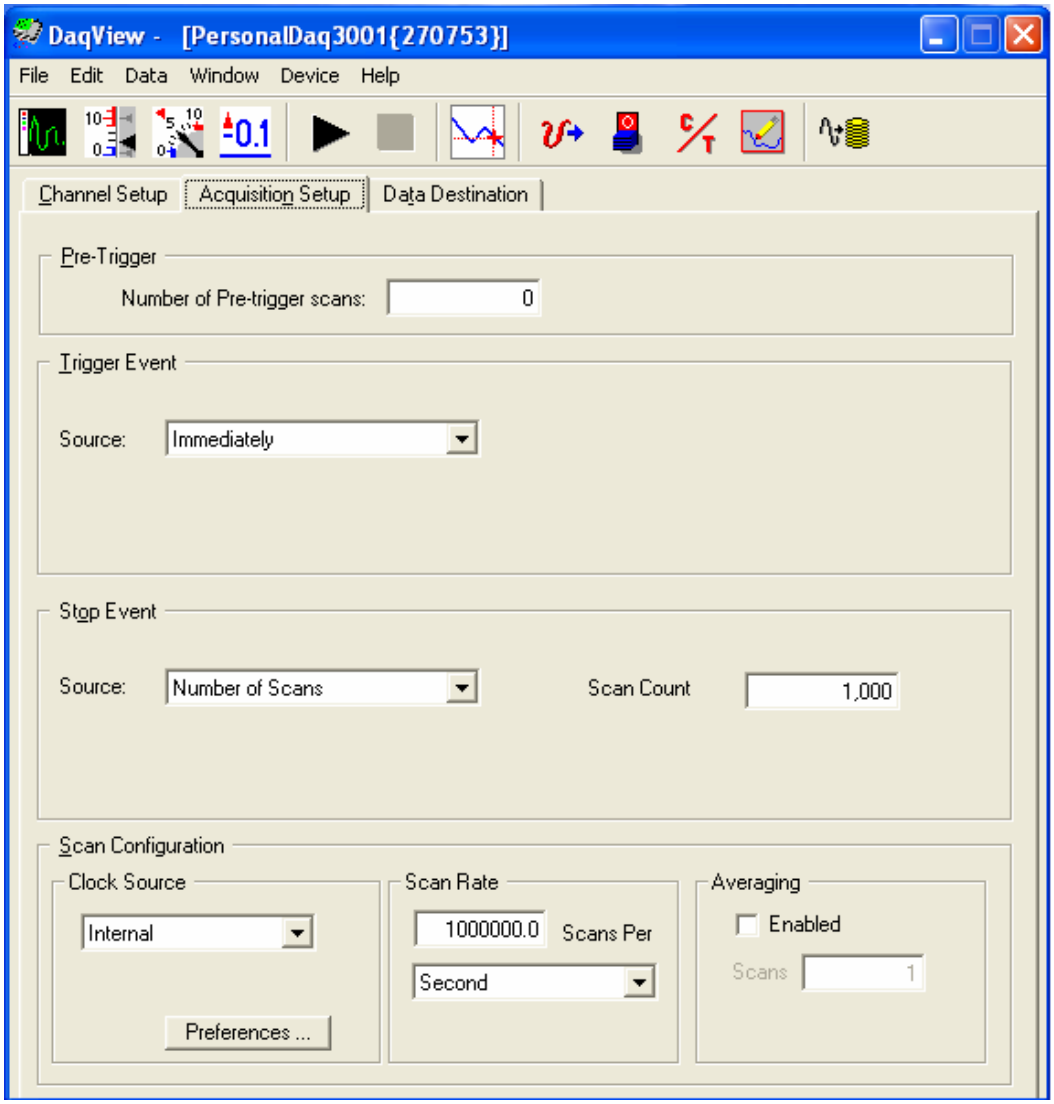


**Figure 28 - Acquisition setup**

A maximum of 1000 analog-to-digital conversions are done per reading. This allows for a minimum velocity measurement of 800 m/s to be measured at a sample length of 35 cm. The maximum speed that can be measured is determined by sampling rate of the hardware. In the case of the IOTech Personal DAQ system used in this project, the maximum sampling rate is one million samples per second over one channel which amounts to a maximum effective velocity measurement of 8000 m/s. This is well within the range of most rock types in South Africa which vary between 1500 m/s and 7000 m/s.

Since the IOTech Personal DAQ system is a 16 channel system it must be setup in order to record on one channel only (Figure 29). This is done

because the bandwidth is divided between the channels that are recording. The more channels recording, the slower the sampling rate per channel will be. If only one channel is recording it can use the full bandwidth of the system (i.e. one million samples per second). Since this system requires only one recording channel, only one is used.

The gain can also be set in this window. All the channel gains can be set individually between 1 and 100. This is useful for weaker signals that generate higher signal to noise ratios at lower gain settings. The output data is scaled back to actual voltage values.

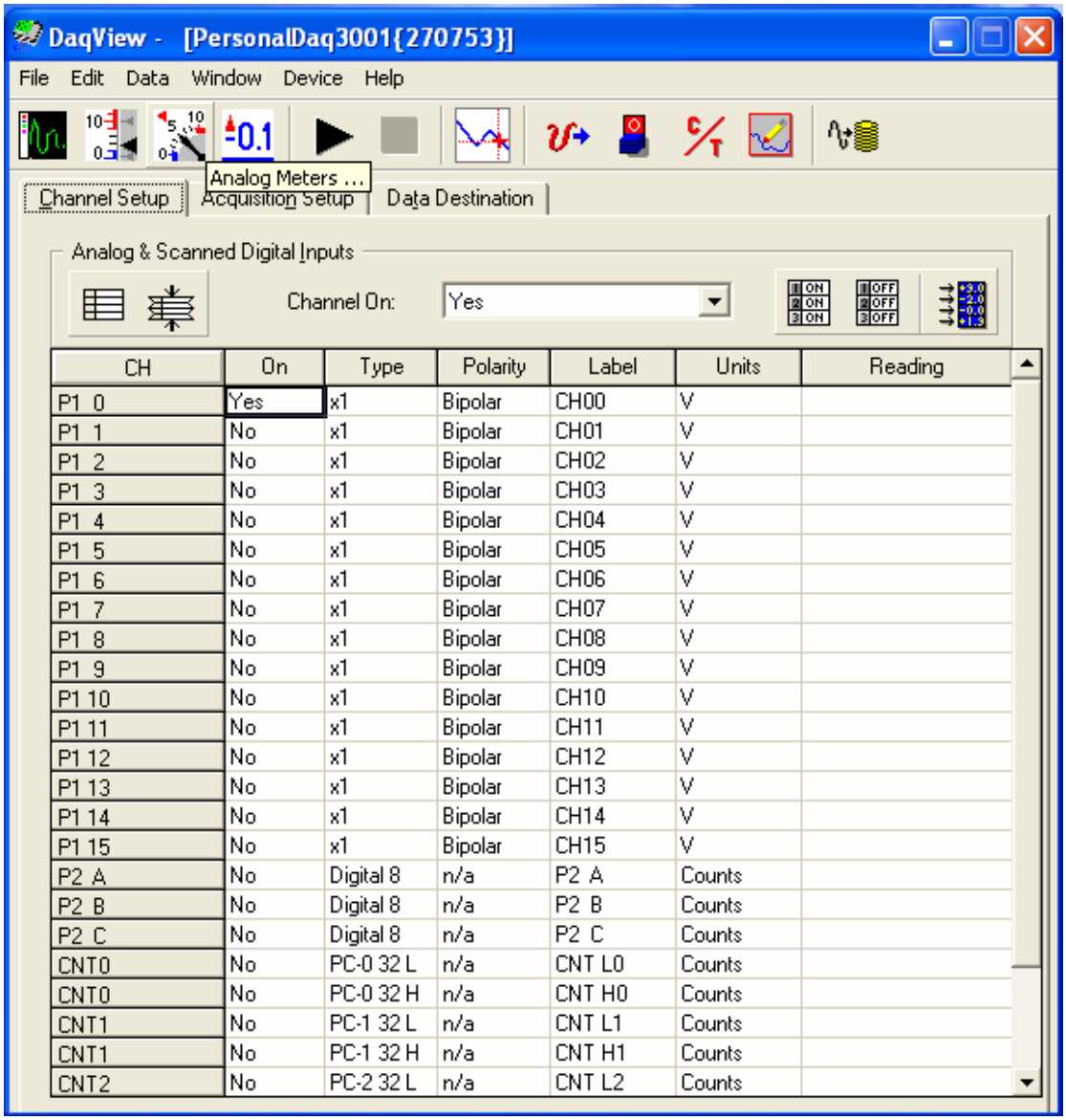


| CH | On | Type | Polarity | Label | Units | Reading |
|---|---|---|---|---|---|---|
| P1 0 | Yes | x1 | Bipolar | CH00 | V | |
| P1 1 | No | x1 | Bipolar | CH01 | V | |
| P1 2 | No | x1 | Bipolar | CH02 | V | |
| P1 3 | No | x1 | Bipolar | CH03 | V | |
| P1 4 | No | x1 | Bipolar | CH04 | V | |
| P1 5 | No | x1 | Bipolar | CH05 | V | |
| P1 6 | No | x1 | Bipolar | CH06 | V | |
| P1 7 | No | x1 | Bipolar | CH07 | V | |
| P1 8 | No | x1 | Bipolar | CH08 | V | |
| P1 9 | No | x1 | Bipolar | CH09 | V | |
| P1 10 | No | x1 | Bipolar | CH10 | V | |
| P1 11 | No | x1 | Bipolar | CH11 | V | |
| P1 12 | No | x1 | Bipolar | CH12 | V | |
| P1 13 | No | x1 | Bipolar | CH13 | V | |
| P1 14 | No | x1 | Bipolar | CH14 | V | |
| P1 15 | No | x1 | Bipolar | CH15 | V | |
| P2 A | No | Digital 8 | n/a | P2 A | Counts | |
| P2 B | No | Digital 8 | n/a | P2 B | Counts | |
| P2 C | No | Digital 8 | n/a | P2 C | Counts | |
| CNT0 | No | PC-0 32 L | n/a | CNT L0 | Counts | |
| CNT0 | No | PC-0 32 H | n/a | CNT H0 | Counts | |
| CNT1 | No | PC-1 32 L | n/a | CNT L1 | Counts | |
| CNT1 | No | PC-1 32 H | n/a | CNT H1 | Counts | |
| CNT2 | No | PC-2 32 L | n/a | CNT L2 | Counts | |

**Figure 29 - Channel Setup**

The DAQView software also allows for the generation of the ultrasound pulse data that the IOTech DAQ system uses to drive the transmitting transducer. The pulse is set to 10 kHz and has an output voltage swing of +- 10 V (Figure 30). This is a large enough voltage to drive the transducer. The system is set to start transmitting the pulse as soon as the user tells the system to record data.

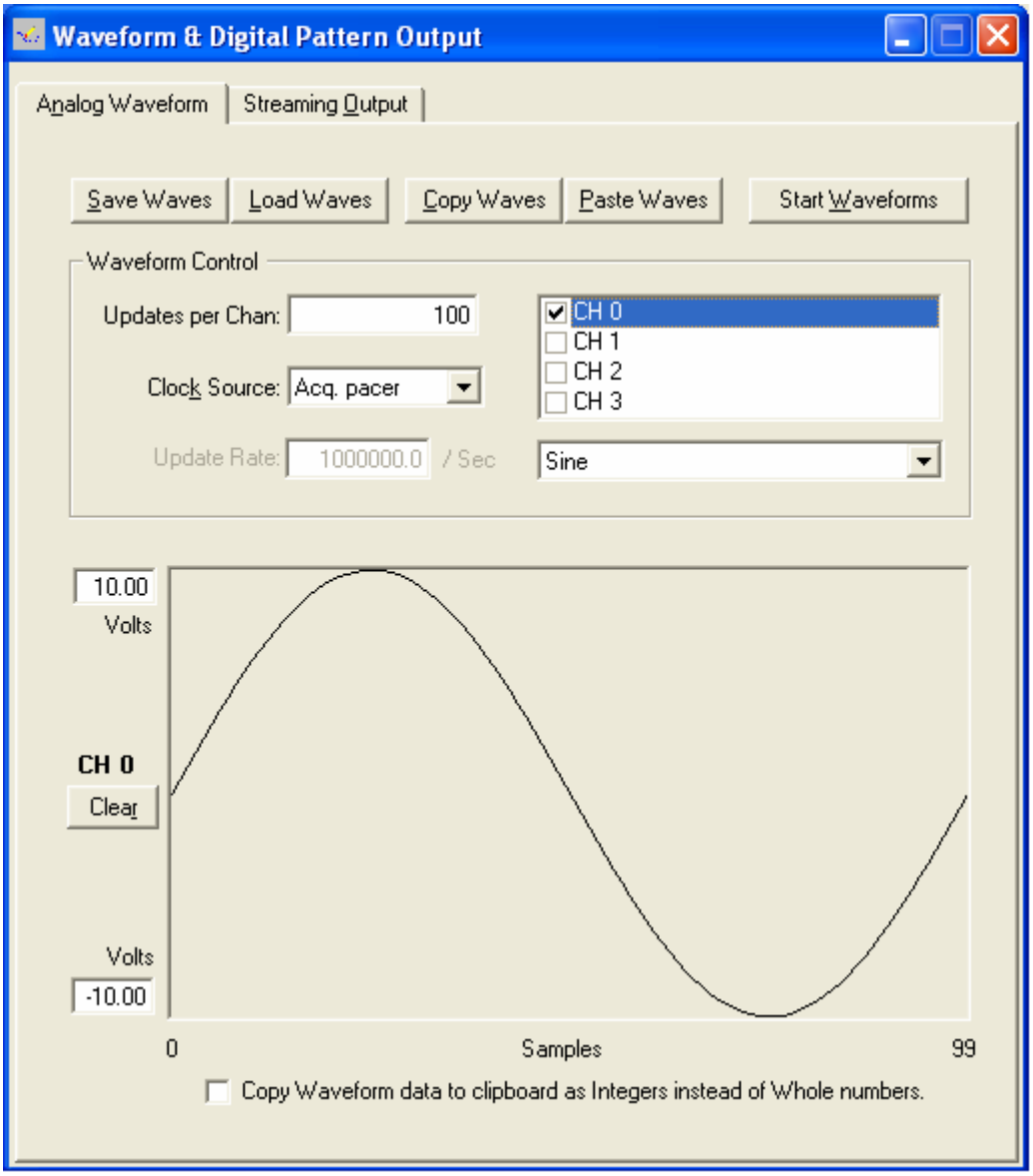


**Figure 30 - Waveform Generator**

Figure 31 shows the software developed for the project. This software imports the text file time-of-flight data captured by the DAQ system and analyses it for velocity values of the sample.

Before an analysis can be done, the user must enter a number of sample parameters, such as sample dimensions, density and porosity. There are a few values which are available that are set to default values. An example of this is the system sample rate and the gravitational constant.

The sample dimensions that the software requires, is the length and diameter of the sample. This is necessary for the calculation of the volume of the sample as well as the calculation of the actual compressional and shear velocities of the sample. The mass of the sample is also required to calculate the density of the sample in conjunction with the calculated sample volume.

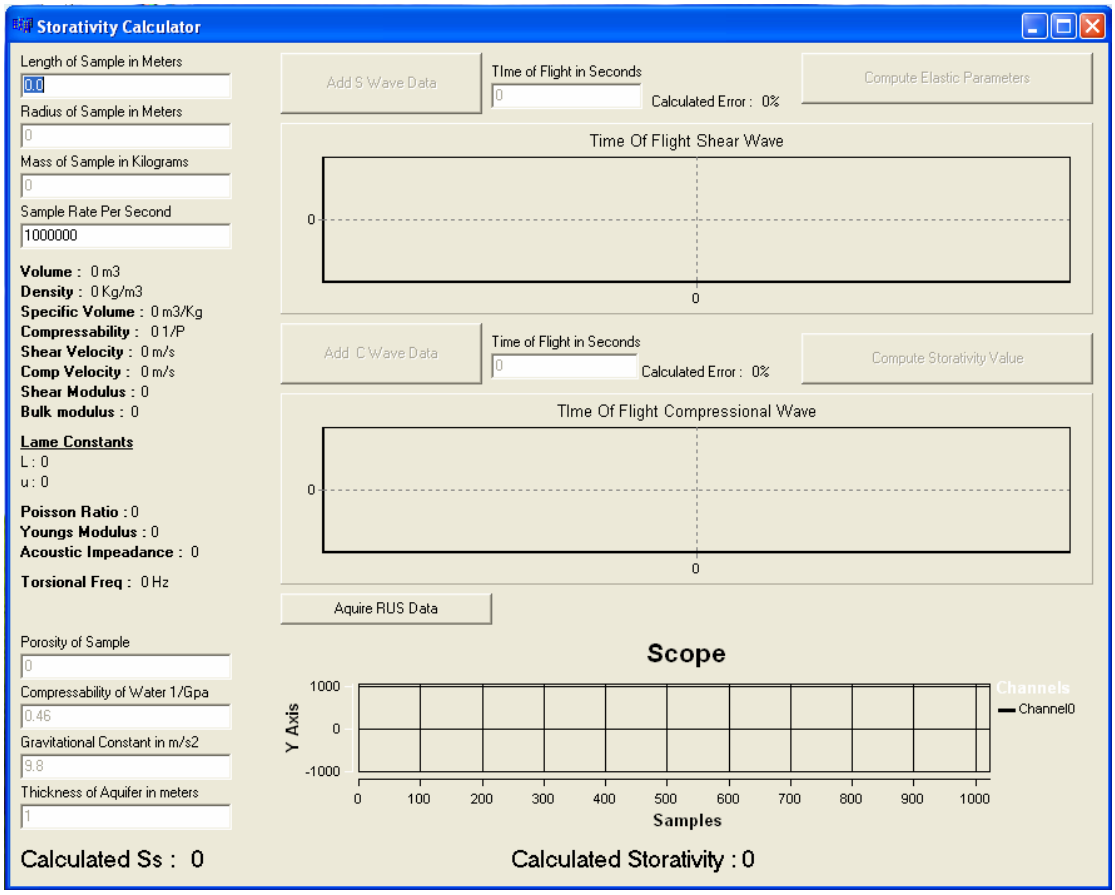


**Figure 31 - Analysis software**

Once these basic parameters are used as input into the software, the software will allow the user to import the time-of-flight data in text form. The shear wave data are imported first. A line trace is displayed in the shear velocity window. The user must then select the point on the trace where the data shows sine wave oscillations. This indicates the time it took the shear wave to travel along the length of the sample. This time value is displayed in the software and is used to calculate the shear wave velocity for the sample. The software then allows the user to repeat the process for the compressional wave time-of-flight data. The user selects the time the data starts oscillating and the software uses this time to calculate the compressional wave velocity for the sample. Figure 32 shows the imported data for the shear and compressional wave velocity calculations.

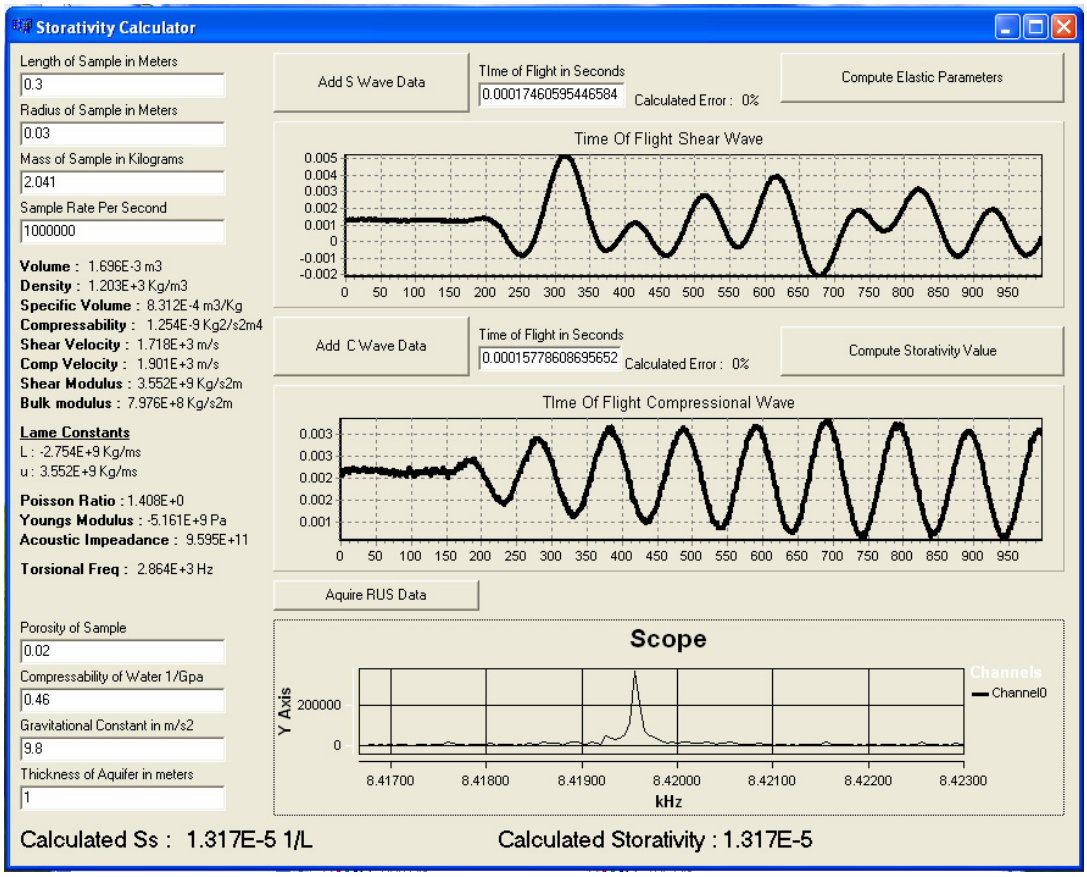


**Figure 32 - Imported Data**

The trace data clearly shows where the ultrasound waves reached the receiving transducers. Once the velocity data for the sample is calculated, the elastic parameters can be calculated. This is done by clicking the “calculate elastic parameters” data button. All the calculated data values are displayed in the window and include:

- **Sample volume**

$$Volume = 2\pi \times Radius^2 \times Length$$

- **Sample density**

$$Density = \frac{Mass}{Volume}$$

- **Specific volume**

$$SpecificVolume = \frac{Volume}{Mass}$$

- **Sample compressibility**

$$Compressibility = \frac{1}{BulkModulus}$$

- **Shear velocity**

$$ShearVelocity = \frac{LengthofSample}{TimeofShearFlight}$$

- **Compressional velocity**

$$CompressionalVelocity = \frac{LengthofSample}{TimeofCompressionalFlight}$$

- **Shear Modulus**

$$G = V_s^2 \times \rho$$

G = Shear modulus
Vs = Shear velocity
ρ = Density of the rock sample

- **Bulk Modulus**

$$K = V_p^2 \rho - \frac{4G}{3}$$

K = Bulk modulus
Vp = Compressional wave velocity
G = Shear modulus
ρ = Density of the rock sample

- **Lamé Constants**

$$\lambda = \rho(v_p^2 - 2v_s^2)$$

$$\mu = \rho v_s^2$$

*E* = Young's modulus
*G* = shear modulus
K = bulk modulus
ρ = density
Vp = P-wave speed
Vs = *S*-wave speed

- **Poisson ratio**

$$v = \frac{1}{2} \frac{(\frac{V_p}{V_s})^2 - 2}{(\frac{V_p}{V_s})^2 - 1}$$

λ Lamé constant
Vp is the *P*-wave speed
Vs is the *S*-wave speed

- **Young's Modulus**

$$E = \frac{\mu(3\lambda + 2\mu)}{\lambda + u}$$

μ and λ = Lamé constants.

- **Torsional resonant frequency**

$$f = \frac{n}{2L}\sqrt{\frac{G}{\rho}}$$

f = Resonant Torsional mode frequency
n = 1 for lowest natural frequency
L = Length of the sample
G = Shear modulus
ρ = Density of the rock sample

- **Specific Storativity**

$$S_s = \rho g(\alpha + \eta\beta)$$

ρ = density of water
g = gravitational constant
$\alpha$ = compressibility of the rock
β = compressibility of the water
η = porosity of the rock

All the equations described above have been discussed in previous chapters. The scope trace on the window is used to generate a RUS frequency sweep as well as record that sweep. This is done by attaching the transducers to the computer sound card; one to the audio out port and one to the line in port. Once the cables are connected, the “acquire RUS data” button on the software window can be clicked to generate and record the frequency sweep. This process takes about fifteen seconds to complete. Once the sweep is complete, an automatic process in the software will convert the data to its frequency domain and display it on the scope window.

The scope window can be used to zoom into specific frequency ranges of the recorded data to better evaluate the resonant frequency peaks. The Torsional mode resonant frequency should be compared to the resonant frequency peaks on the scope window. If there is no resonant frequency at the point predicted, then the sample is a bad one and another should be selected and retested. If it is, then an accurate value for the elastic parameter has been calculated.

# Chapter 7 - Fracture Model

The purpose of the fracture model discussed in this chapter is to demonstrate one of the currently available applications of the linear elastic parameters determined by the apparatus in this paper. Since the Young's modulus for linear elasticity of a sample can be determined by using the apparatus developed in this paper, it can be directly applied to the aquifer deformation model developed by Botha and Cloot (2004) for the WRC. A full mathematical description for this model can be found in Botha and Cloot (2004). Since a full description of the model is available, this report is will not be discussed here. The Botha and Cloot (2004) model is used to determine the elastic deformations induced in an aquifer and fracture by the application of stresses to the aquifer, by pumping of a borehole. The model simulates both linear and non-linear elastic deformation of the aquifer.

For the purposes of this paper, the model was run with the linear elastic parameters determined for the average Young's modulus of the campus aquifer. This was done by adding the Young's moduli for all the stone types in the campus aquifer and then dividing by the number of samples added.

For the purposes of this study, the same hydrological data (Table 1), as well as the same geological model (Figure 33) was used in this simulation as in the original study.

**Table 1 - Hydraulic conductivity parameters (Botha and Cloot, 2004)**

| Depth (m) | K (ms-1) | |
|---|---|---|
| | Krr | Kzz |
| 0.00 | $1.04 \times 10^{-6}$ | $1.00 \times 10^{-8}$ |
| 5.00 | $1.04 \times 10^{-7}$ | $1.00 \times 10^{-9}$ |
| 10.00 | $3.01 \times 10^{-6}$ | $1.00 \times 10^{-10}$ |
| 15.00 | $6.21 \times 10^{-8}$ | $1.95 \times 10^{-11}$ |
| 17.00 | $2.80 \times 10^{-7}$ | $1.12 \times 10^{-11}$ |
| 20.00 | $2.24 \times 10^{-6}$ | $1.12 \times 10^{-10}$ |
| 20.75 | $2.33 \times 10^{-5}$ | $4.64 \times 10^{-9}$ |
| 20.95 | $2.33 \times 10^{-4}$ | $4.64 \times 10^{-9}$ |
| 21.00 | $2.33 \times 10^{-4}$ | $4.64 \times 10^{-9}$ |
| 21.05 | $2.33 \times 10^{-4}$ | $4.64 \times 10^{-9}$ |
| 21.25 | $2.33 \times 10^{-5}$ | $4.64 \times 10^{-9}$ |
| 22.00 | $2.87 \times 10^{-7}$ | $9.64 \times 10^{-10}$ |
| 25.00 | $4.16 \times 10^{-7}$ | $9.64 \times 10^{-10}$ |
| 32.50 | $5.04 \times 10^{-8}$ | $9.83 \times 10^{-10}$ |
| 40.00 | $6.20 \times 10^{-8}$ | $9.83 \times 10^{-10}$ |
| Fracture | $9.00 \times 10^{-3}$ | $9.00 \times 10^{-3}$ |

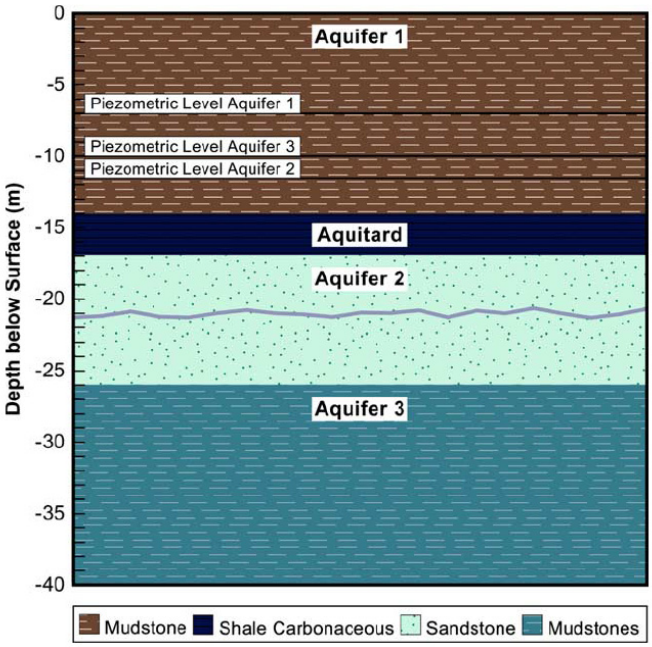


**Figure 33 - Campus model (Botha and Cloot, 2004)**

Figure 33 shows the model used to simulate the campus aquifer. The data for this model was taken from Botha and Cloot's original simulation of the campus aquifer. The Young's modulus is taken as the average of the sampled moduli of the campus formation. This value was found to be 3.1 x $10^8$ which is very close to the value of 7.25 x $10^7$ used in the original simulation by Botha and Cloot (2004). An average storativity value of 1 x $10^{-4}$ was used throughout the aquifer. A fracture of 9 x $10^{-3}$ m/s hydraulic conductivity is located at a depth of 21 meters. The first simulation was conducted using the linear elastic model (Figure 34). In this model no residual effects are simulated and deformations are not permanent.

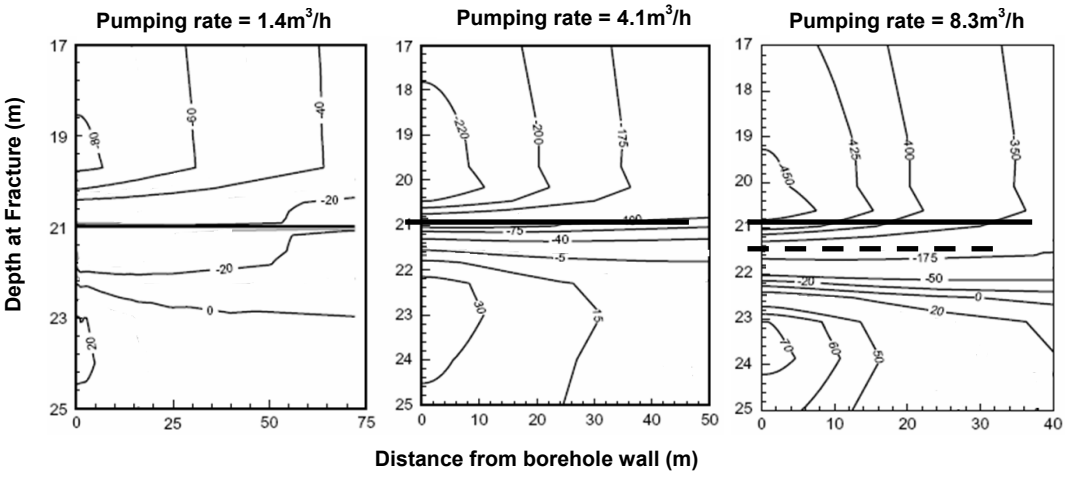


**Figure 34 - Linear elastic deformation simulation**

The simulation was done at different pumping rates to show the effect that over stressing of the borehole will have on the deformation of the fracture. The same pumping rate simulations were used as in Botha and Cloot's simulation, namely, 1.4, 4.1 and 8.3 $m^3$/h. It shows a concentration of deformations at the fracture. These deformations are however linear and uniform.

The non-linear model was used to simulate the effect that extreme stress placed on the fracture would do to the aquifer. As before, the same pumping rates were used as that of Botha and Cloot (2004). The data for the non-linear Hooke function used to determine the Young modulus for a given stress a given node in the model, was taken from Botha and Cloot's simulation data of the campus test site. Figure 35 shows the simulated non-linear deformation of the fracture. It shows a highly deformed fracture that is not uniform as is the case in the linear simulation.

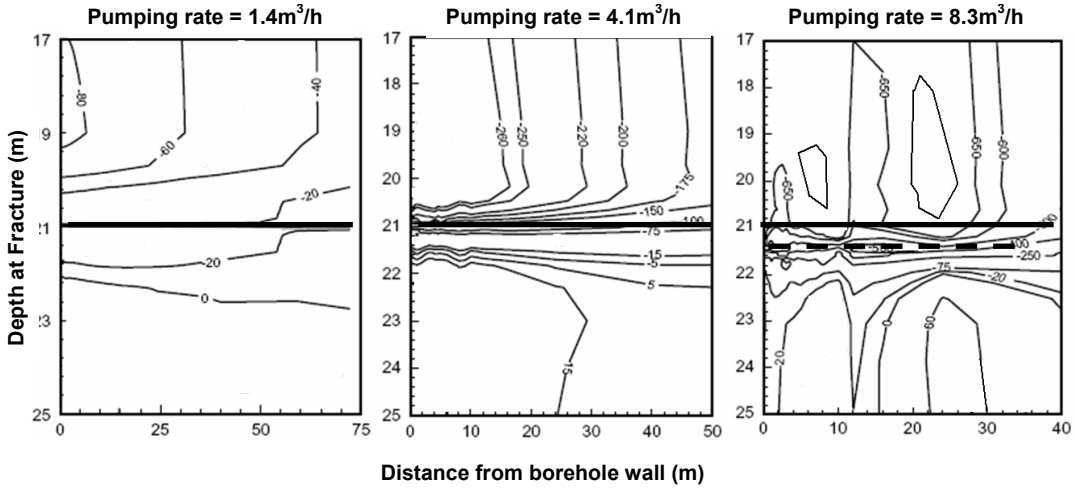


**Figure 35 - Non-linear elastic deformation simulation**

Another simulation feature that was also seen in the original study is that the majority of the deformation occurs in the area of the bottom of the fracture. As before the model indicates severe deformation of the aquifer and fracture on the campus test site when put under pumping stress. This confirms Botha and Cloot's original position that over stressing of a borehole by over pumping will have adverse affects on the aquifer and the fractures running through it. This confirms the need for the proper pump testing of supply boreholes, so that there life span and efficiency can be optimized (Botha and Cloot, 2004).

# Chapter 8 - Experimental Results

## *8.1 Test Samples*

The test samples that were used in the evaluation of the system are shown in Figure 36.


**Figure 36 - Test sample**

Some of the samples used are half cylinder core cuts. The test indicates that the system works well with these cores as well. Table 2 shows the dimensions and properties of the test samples used in this study. A varied selection of rock types where used to evaluate the system. The results are discussed below. Porosity values of two to seven percent were used.

**Table 2 - Sample dimensions and characteristics**

| Rock Type | Length | Radius | Volume | Mass | Density | Specific Vol. |
|---|---|---|---|---|---|---|
| | m | m | m³ | Kg | Kg/m³ | m³/Kg |
| **TMG Sandstone** | 0.097 | 0.027 | 4.44E-04 | 5.87E-01 | 1.32E+03 | 7.57E-04 |
| **Schist** | 0.240 | 0.020 | 6.03E-04 | 8.91E-01 | 1.48E+03 | 6.77E-04 |
| **Quartzite** | 0.176 | 0.020 | 4.42E-04 | 6.54E-01 | 1.48E+03 | 6.76E-04 |
| **Gneiss** | 0.104 | 0.020 | 2.61E-04 | 3.73E-01 | 1.43E+03 | 7.01E-04 |
| **Campus Shale** | 0.215 | 0.030 | 1.22E-03 | 1.51E+00 | 1.25E+03 | 8.03E-04 |
| **Granite** | 0.354 | 0.015 | 2.50E-04 | 3.03E-01 | 1.21E+03 | 8.26E-04 |
| **Dolerite** | 0.150 | 0.015 | 1.06E-04 | 1.51E-01 | 1.42E+03 | 7.02E-04 |
| **Dolomite** | 0.164 | 0.015 | 1.16E-04 | 1.63E-01 | 1.41E+03 | 7.11E-04 |
| **Campus Sandstone** | 0.300 | 0.030 | 1.70E-03 | 2.04E+00 | 1.20E+03 | 8.31E-04 |

## *8.2 Time-of-flight Results*

Table 3 shows the time-of-flight results for the test samples. The specific storativity results were calculated with the velocity data indicated and a porosity value given in the table for each sample.

**Table 3 - Time-of-flight results**

| Rock Type | Specific Storativity | Shear Velocity | Compressional Velocity |
|---|---|---|---|
| | 1/L | m/s | m/s |
| **TMG Sandstone** | 1.295E-06 | 1936 | 4879 |
| **Schist** | 6.459E-06 | 1617 | 2163 |
| **Quartzite** | 1.318E-06 | 2331 | 4806 |
| **Gneiss** | 1.048E-06 | 2590 | 7445 |
| **Campus Shale** | 1.244E-05 | 1090 | 1559 |
| **Granite** | 1.786E-06 | 2409 | 4107 |
| **Dolerite** | 1.408E-06 | 2631 | 4773 |
| **Dolomite** | 1.148E-06 | 2881 | 6262 |
| **Camp Sandstone** | 2.009E-05 | 1643 | 2011 |

## *8.3 RUS results*

The RUS data is shown in Table 4. The calculated fundamental torsional resonance frequency is compared to the actual fundamental torsional frequency recorded by the system for each sample. As can be seen in Table 7 the calculated analytical value is very close to the actual value recorded. This indicates that all of the samples are relatively homogeneous with very few impurities or imperfections as the highest and average values for specific storativity are approximately the same value.

**Table 4 - RUS Results**

| Rock Type | Calculated Resonance Frequency | Recorded Resonance Frequency |
|---|---|---|
| | Hz | Hz |
| **TMG Sandstone** | 94 | 95 |
| **Schist** | 194 | 190 |
| **Quartzite** | 205 | 202 |
| **Gneiss** | 135 | 130 |
| **Campus Shale** | 117 | 120 |
| **Granite** | 426 | 430 |
| **Dolerite** | 197 | 200 |
| **Dolomite** | 236 | 237 |
| **Camp Sandstone** | 246 | 250 |

## *8.4 Summary of Results*

Table 5 shows the most important elastic parameters calculated by the system, namely, the bulk and shear modulus. Additional parameters that are calculated are shown in Table 6.

**Table 5 - Elastic parameter results**

| Rock Type | Shear Modulus | Bulk Modulus | Compressibility | Lamé Variable μ |
|---|---|---|---|---|
| | Kg/s²m | Kg/s²m | Pa | |
| **TMG Sandstone** | 4.952E+09 | 2.485E+10 | 4.025E-11 | 4.952E+09 |
| **Schist** | 3.862E+09 | 1.761E+09 | 5.678E-10 | 3.862E+09 |
| **Quartzite** | 8.034E+09 | 2.344E+10 | 4.266E-11 | 8.034E+09 |
| **Gneiss** | 9.573E+09 | 6.633E+10 | 1.508E-11 | 9.573E+09 |
| **Campus Shale** | 1.480E+09 | 1.054E+09 | 9.488E-10 | 1.480E+09 |
| **Granite** | 7.027E+09 | 1.106E+10 | 9.046E-11 | 7.027E+09 |
| **Dolerite** | 9.858E+09 | 1.930E+10 | 5.181E-11 | 9.858E+09 |
| **Dolomite** | 1.167E+10 | 3.958E+10 | 2.527E-11 | 1.167E+10 |
| **Camp Sandstone** | 3.248E+09 | 5.352E+08 | 1.868E-09 | 3.248E+09 |

**Table 6 - Additional parameter results**

| Rock Type | Lamé Variable λ | Young's Modulus | Poisson's Ratio | Acoustic Impedance |
|---|---|---|---|---|
| | | Pa | | |
| **TMG Sandstone** | 2.155E+10 | 1.393E+10 | 4.485E-01 | 3.283E+13 |
| **Schist** | 8.136E+08 | 6.694E+09 | 3.640E-01 | 2.602E+12 |
| **Quartzite** | 1.808E+10 | 2.163E+10 | 4.091E-01 | 3.465E+13 |
| **Gneiss** | 5.995E+10 | 2.740E+10 | 4.630E-01 | 9.466E+13 |
| **Campus Shale** | 6.759E+07 | 3.024E+09 | 4.186E-02 | 1.312E+12 |
| **Granite** | 6.370E+09 | 1.740E+10 | 3.223E-01 | 1.339E+13 |
| **Dolerite** | 1.273E+10 | 2.527E+10 | 3.604E-01 | 2.749E+13 |
| **Dolomite** | 3.179E+10 | 3.188E+10 | 4.225E-01 | 5.565E+13 |
| **Camp Sandstone** | 1.630E+09 | 3.223E+09 | 1.341E+02 | 6.439E+11 |

# Chapter 9 - Summary

Although the study shows that specific storativity can be accurately determined by this system, it is important to realise that this system is also dependant on a number of things. The first is that the samples used in the testing process must be prepared very carefully. Attention to the cutting edge is essential, the flatter the cut, the better the result. The samples must also be selected to be as homogeneous as possible to avoid discrepancies between the time-of-flight and RUS results. The length of the sample must also be kept as long as possible to improve the sampling error induced. Testing should be carried out in a noise-free environment to ensure results are not false ones and all results should be checked at least twice to verify consistency.

Although the system gives very good results due to the dual checking of time-of-flight and RUS methods results to determine a final result, it is always a good idea to check the results against average known specific storativity values for the rock types under test. This will give the user an idea of whether the results obtained are realistic or not and may necessitate the need to test the sample again or use a different sample to compare values to.

# References


Botha JF and Cloot AHJ (2004). Karoo Aquifers: Deformations, hydraulic and mechanical properties. WRC Report: 936/1/04. Water Research Commission, Pretoria

Botha JF and Cloot AHJ (2004). Deformations and the Karoo aquifers of South Africa. Advances in Water Resources 27, 383 – 398.

Boyd T (2003). Introduction to Geophysics Short Course. Retrieved March 1, 2007, from Colorado School of Mines, Web site: http://gretchen.geo.rpi.edu/roecker/AppGeo96/lectures/gravity/main.html.

Choudhari NK, Kumar A, Kumar Y and Gupta R (2002) Evaluation of elastic moduli of concrete by ultrasonic velocity. National Seminar of Indian Society for Non-Destructive Testing 5 (12), 1-4.

Hermance J (2003). Storage Properties of Aquifers. Retrieved March 1, 2007, from Brown University, Web site: http://www.brown.edu/Courses/GE0158/ge158web/classsupplements/2003/StoragePropertiesOfAquifers.ppt.

Jennings D and Flint A (1995). Introduction to Medical Electronics Applications. Butterworth-Heinemann, USA, 51-82.

Leisure RG and Willis FA (1997). Resonant Ultrasound spectroscopy. Journal of Physics 9, 601 – 629.

Madeira MM, Bellis SJ and Beltran LAA (1999). High-performance computing for real-time spectral estimation. Control Engineering Practice 7 (5), 679-686.

Powis RL and Schwartz RA (1998). Practical Doppler ultrasound for the clinician. Gale Group, USA. 177p.

Wang YC and Lakes RS (2003). Lakes Resonant ultrasound spectroscopy in shear mode. Review of scientific instruments 74 (5) 1371-1373.

Wayne R, Hykes DL and Hedrick WR (2005). Ultrasound physics and instrumentation. Mosby Year Book, St. Louis. 464p.

Weisstein E (2007). World of physics. Retrieved March 1, 2007, from Wolfram Research, Web site: http://scienceworld.wolfram.com/physics/

Zadler B and Le Rousseau JHL (2003). Resonant Ultrasound spectroscopy: theory and application. Physical Acoustics Laboratory and Center for wave phenomena, Colorado school of mines. 17p.

Zadler B, Le Rousseau JHL, Scales JA and Smith ML (2004). Resonant Ultrasound spectroscopy: theory and application. Geophysics Journal International 156, 154-169.